Players and mechanisms involved in the biogenesis of cyanobacterial extracellular vesicles

Delfim Cardoso

Mestrado em Aplicações em Biotecnologia e Biologia Sintética

Departamento de Biologia, Departamento de Química e Bioquímica

2021

Orientador

Doutor Paulo Oliveira, Investigador Auxiliar no Grupo Bioengineering & Synthetic Microbiology i3S/IBMC, Universidade do Porto
Professor Auxiliar Convidado da Faculdade de Ciências da Universidade do Porto

Coorientador

Professora Doutora Paula Tamagnini, Professora Associada da Faculdade de Ciências da Universidade do Porto; Líder do grupo Bioengineering & Synthetic Microbiology i3S/IBMC, Universidade do Porto

Todas as correções determinadas pelo júri, e só essas, foram efetuadas.
O Presidente do Júri,

Porto, _____/_____/_____

Agradecimentos

A presente tese de mestrado não poderia ter sido realizada sem o incansável companheirismo e apoio de várias pessoas, aos quais estou eternamente grato.

À Professora Paula Tamagnini, por me ter aceite na sua equipa e por me ter proporcionado uma oportunidade única, onde pude crescer como aluno e como pessoa. Agradeço ainda o acompanhamento no meu percurso académico, desde a minha licenciatura até ao final deste mestrado.

Ao meu orientador, Paulo Oliveira, gostaria de começar por agradecer o **empenho** e **paciência** com que me acompanhaste durante a elaboração desta dissertação. Obrigado por todos os ensinamentos que me transmitiste ao longo destes últimos anos, pelas conversas de motivação, mas também pelos momentos em que me chamaste à razão. Foste um verdadeiro modelo a seguir.

Ao Stevee e ao Jorge, meus companheiros da equipa “Bolinha”, obrigado por me terem apoiado durante esta aventura, e por mostrarem o que é trabalho em equipa. Com vocês foi possível perceber que na seriedade do laboratório podemos ser nós próprio e construir boas amizades.

Agradeço, ainda, a todos os membros do grupo Bioengineering & Synthetic Microbiology, pela simpatia com que me receberam e por terem estado sempre prontos para me ajudar. Obrigada também por irem tolerando o meu sentido de humor pouco convencional e por se preocuparem com a minha saúde alimentar.

À minha namorada, Inês, pelo amor, carinho e apoio com que me acompanhas há vários anos, e em particular durante os últimos meses. Foste essencial nesta aventura e sei que posso contar contigo para todas as que vierem.

Por último, mas não menos importante, quero agradecer à minha família, pela preocupação e por estarem sempre prontos a ajudar. Agradeço em especial aos meus pais, pelo amor, pelo carrinho, e pelo apoio incondicional que sempre me deram.

Este trabalho foi financiado pelo Fundo Europeu de Desenvolvimento Regional (FEDER) através do Programa Operacional de Competitividade e Internacionalização (COMPETE 2020), Portugal 2020, e por fundos nacionais através da Fundação para a Ciência e a Tecnologia / Ministério da Ciência, Tecnologia e Ensino Superior através do projeto POCI-01-0145-FEDER-029540 (PTDC/BIA-OUT/29540/2017).

Abstract

Extracellular vesicles (EVs) are nano-sized spherical structures released by all living organisms. Biotechnology has long been interested in bacterial EVs, particularly as drug delivery systems, and as platforms for the development of vaccines. To engineer bacterial strains that can produce large amounts of EVs with tailored cargo, a comprehensive knowledge of EVs formation and release is needed. Cyanobacteria are photosynthetic microorganisms that have been increasingly used as bio-factories, representing a solid platform towards implementing a greener industrial transformation. However, several aspects related to composition, biogenesis and biological roles of EVs are poorly studied in these prokaryotic microorganisms, which limits their use in biotechnological applications. Therefore, the main goal of this work was to identify players and mechanisms involved in cyanobacterial EVs biogenesis. Having as starting point the models proposed for the formation and release of EVs in Gram-negative bacteria, here, two approaches were followed to address the mechanisms underlying EVs production in the model cyanobacterium *Synechocystis* sp. PCC 6803: 1) modulation of the outer membrane-peptidoglycan links; and 2) modulation of periplasmic pressure by accumulation of heterologous proteins. To address these topics, a set of cyanobacterial mutant strains were studied, including knockout mutants and strains expressing the reporter protein sfGFP. Cultures' growth analyses, identification of proteomic adaptations in response to target gene deletion, and isolation and characterization of EVs, were carried out to give a comprehensive view of the investigated mechanisms. The results show that one of the highly abundant outer membrane proteins may have dual biological role, as it may work as a porin for the selective passage of ions and contribute to the overall linkage between the outer membrane and the underlying peptidoglycan layer. In agreement, the corresponding knockout mutant was found to release substantially more EVs than the wild-type strain. Moreover, it is shown that it is possible to tailor the cyanobacterial EVs protein cargo with a heterologous protein, and that EVs production correlates to the amount of protein being expressed and translocated to the periplasm. Altogether, these findings suggest that cyanobacterial EVs biogenesis mechanisms follow the basic principles proposed for other Gram-negative bacteria, and expand the spectrum of biotechnological applications possible with cyanobacteria and their EVs.

Keywords: *Synechocystis* sp. PCC 6803, Extracellular vesicles (EVs), Outer membrane protein, Slr1908, EVs protein customization.

Resumo

As vesículas extracelulares são nano-estruturas esféricas virtualmente libertadas por todos os organismos vivos. Diversas áreas da Biotecnologia têm apresentado ao longo dos últimos anos interesse nas vesículas de origem bacteriana, particularmente como plataformas para o transporte de fármacos e para o desenvolvimento de vacinas. De forma a desenvolver estirpes bacterianas que sejam capazes de produzir grandes quantidades de vesículas com conteúdo customizado é necessário um conhecimento abrangente dos mecanismos de formação e libertação destas vesículas. As cianobactérias são microrganismos fotossintéticos que têm vindo a ser progressivamente mais utilizados como bio-fábricas, representando uma sólida alternativa para a transição e implementação de práticas mais verdes em diferentes sectores na indústria. No entanto, vários aspetos relacionados com a composição, biogénese e funções biológicas das vesículas foram pouco estudados nestes organismos procarióticos, o que limita as suas potenciais aplicações. Assim, o principal objetivo deste trabalho foi a identificação de intervenientes e de mecanismos envolvidos na biogénese de vesículas em cianobactérias. Tendo como ponto de partida os modelos propostos para a formação e libertação de vesículas em bactérias Gram-negativas, duas abordagens foram aqui seguidas que visam os mecanismos subjacentes à produção de vesículas na cianobactéria-modelo *Synechocystis* sp. PCC 6803: 1) modulação das ligações entre a membrana externa e o peptidoglicano; 2) modulação da pressão periplasmática através da acumulação de proteínas heterólogas. De modo a abordar estes tópicos, um conjunto de estirpes cianobacterianas mutantes foram estudadas, as quais incluem mutantes de deleção e estirpes que expressam a proteína repórter sfGFP. Análises do crescimento de culturas, identificação de adaptações proteómicas em resposta à deleção de um gene de interesse, e isolamento e caracterização de vesículas, foram realizadas de forma a recolher dados que garantissem uma visão abrangente dos processos em estudo. Os resultados obtidos mostram que uma das proteínas mais abundantes de membrana externa poderá assumir dupla função biológica, uma vez que atua como uma porina para a passagem seletiva de iões, e contribui para o conjunto total de ligações entre a membrana externa e a camada de peptidoglicano subjacente. De modo concordante, o respetivo mutante de deleção demonstrou libertar substancialmente mais vesículas do que a estirpe selvagem. Mais ainda, foi demonstrado que é possível personalizar o conteúdo de vesículas de cianobactérias com proteínas heterólogas, e que a produção de vesículas está relacionada com a quantidade de proteína heteróloga que é expressa e transportada para o periplasma. De uma forma geral, estas evidências sugerem que os mecanismos

de biogénese de vesículas em cianobactérias seguem os mesmos princípios básicos propostos para outras bactérias Gram-negativas, e expande o leque de possíveis aplicações biotecnológicas usando cianobactérias e as suas vesículas.

Palavras chave: *Synechocystis* sp. PCC 6803, Vesículas extracelulares, Proteínas de membrana externa, Slr1908, Customização proteica de vesículas extracelulares.

Index of content

Agradecimentos I

Abstract III

Resumo V

Index of content VII

List of tables and figures IX

List of abbreviations XI

1- Introduction 1

1.1- The Gram-negative bacteria cell envelope 5

1.2- Extracellular vesicles released by Gram-negative bacteria 7

1.3- Extracellular vesicles biogenesis mechanisms in Gram-negative bacteria 9

1.4- Cyanobacteria- past and present 11

1.5- Cyanobacteria- cell envelope and extracellular vesicle production 13

1.6- Objectives 14

2- Material and Methods 15

2.1- Organisms and culture medium 17

2.1.1- Cyanobacterial cultivation and maintenance conditions 17

2.1.2- *Escherichia coli* 18

2.2- Plasmid Construction and mutant generation 18

2.2.1- DNA extraction from *Synechocystis* cultures 19

2.2.2- Polymerase chain reaction (PCR) 19

2.2.3- Agarose gel electrophoresis 20

2.2.4- DNA ligation reactions 21

2.2.5- *E. coli* transformation 21

2.2.6- *Synechocystis* transformation 21

2.3- Characterization of *Synechocystis* mutants 22

2.3.1- Growth rates 22

2.3.2- Outer membrane isolation and purification 22

2.3.3- Extracellular medium isolation and concentration 23

2.3.4- Isolation and characterization of extracellular vesicles 23

2.3.4.1- Transmission electron microscopy 24

2.3.4.2- Nanosight 24

2.3.4.3- Lipopolysaccharide staining 24

2.3.5- Protein analysis and Western blotting 25

2.3.6- Fluorescence measurements 26

2.3.7- Statistical analysis 26

3- Results and Discussion 27

3.1- Modulation of Outer Membrane-Peptidoglycan layer links 29

3.1.1- Identification of candidate proteins and generation of mutant strains 29

3.1.2- Knockout mutants' growth rates in standard culture conditions 32

3.1.3- Outer membrane and cell-free extracellular medium protein content 33

3.1.4- Characterization of the Δ*1908* mutant iron-related phenotype 35

3.1.5- LPS abundance in the cell-free extracellular medium 37

3.1.6- Δ*1908*: a strain with increased vesiculation phenotype 38

3.2- Modulation of periplasmic pressure resulting from the accumulation of heterologous proteins 41

3.2.1- *Synechocystis* mutant strains expressing sfGFP 41

3.2.2- Analysis of intra- and extracellular fluorescence intensity signal 43

3.2.3- Analysis of EVs released by the sfGFP-expressing *Synechocystis* strains 45

4- Conclusion and Future Perspectives 49

5- References 53

List of tables and figures

Table 1. *Synechocystis* sp. PCC 6803 mutant strains used in this work. 17

Table 2. Oligonucleotides used in this work. 20

Figure 1. Ultrastructural details and model of a typical Gram-negative bacterium cell envelope. 7

Figure 2. Types of extracellular vesicles released by Gram-negative bacteria. 8

Figure 3. Mechanisms of EVs production in Gram-negative bacteria. 11

Figure 4. *Synechocystis* sp. PCC 6803 outer membrane proteins homologous to the OmpA protein family and their coding genes. 30

Figure 5. Representation of the pDC1841K plasmid used in this work. 30

Figure 6. Chromosome segregation analysis of the genes encoding proteins containing SLH-OprB-domains. 31

Figure 7. Knockout mutants' growth rates determined in cultures grown in liquid BG11 medium with a 16 h light/ 8 h dark cycle. 32

Figure 8. Analyses of the composition of the knockout mutants' outer membrane and cell-free extracellular medium. 33

Figure 9. *Synechocystis* sp. PCC 6803 wild-type and Δ*1908* mutant growth rates in BG11 medium with modified iron ammonium citrate concentration, under different cultivation setups. 36

Figure 10. Analysis of the lipopolysaccharides (LPS) content in *Synechocystis* sp. PCC 6803 wild-type and knockout mutant strains in cell-free extracellular medium samples. 38

Figure 11. Analysis of the vesiculation capacity of *Synechocystis* sp. PCC 6803 wild-type and Δ*1908* strains. 39

Figure 12. Morphology and size distribution analysis of extracellular vesicles isolated from the *Synechocystis* sp. PCC 6803 wild-type and Δ*1908* mutant based on transmission electron microscopy. 40

Figure 13. Design of the constructs used to generate *Synechocystis* sp. PCC 6803 mutant strains expressing sfGFP and microscopic analysis of the respective fluorescent signal from strain L::Fut. 42

Figure 14. *Synechocystis* sp. PCC 6803 wild-type and sfGFP-expressing mutant strains growth rates determined from cultures grown under standard conditions. 43

Figure 15. Intra- and extracellular sfGFP fluorescence signal determined for the *Synechocystis* sp. PCC 6803 strains L::Fut ($P_{trc.x.lacO}$; with FutA2 signal peptide), R::Fut (P_{rbcL}; with FutA2 signal peptide), L::noSP ($P_{trc.x.lacO}$; without FutA2 signal peptide), and R::noSP (P_{rbcL}; without FutA2 signal peptide). 44

Figure 16. Western blot analysis of the sfGFP protein levels present in the extracellular medium and in isolated vesicles of the sfGFP-expressing *Synechocystis* sp. PCC 6803 mutant strains. 46

Figure 17. Analysis of the vesiculation capacity of the sfGFP-expressing *Synechocystis* sp. PCC 6803 mutants. 47

List of abbreviations

AmpR	Ampicillin resistance cassette
ATP	Adenosine triphosphate
bp	Base pair
CRISPRi (interference)	Clustered regularly interspaced short palindromic repeats (interference)
C-terminal	Carboxyl terminal
DNA	Deoxyribonucleic acid
dNTPs	Deoxynucleotide triphosphate
EDTA	Ethylenediaminetetraacetic acid
EOMVs	Explosive outer membrane vesicles
EVs	Extracellular vesicles
KmR	Kanamycin resistance cassette
LB	Luria-Bertani medium
Lpp	Braun's lipoprotein
LPS	Lipopolysaccharides
mRNA	Messenger ribonucleic acid
OD_{730}	Optical density at 730 nm
OIMVs	Outer-inner membrane vesicles
OMPs	Outer membrane proteins
OMVs	Outer membrane vesicles
OprB	Carbohydrate-selective porin OprB conserved domain
PBS	Phosphate-buffered saline
PCR	Polymerase chain reaction
PQS	*Pseudomonas* quinolone signal
RNA	Ribonucleic acid
SDS	Sodium dodecyl sulphate
sfGFP	Superfolder green fluorescent protein
S-layer	Surface layer
SLH	Surface layer homology domain
SP	Signal peptide

sRNA	Small non-coding ribonucleic acid
TAE	Tris-acetate-EDTA buffer
TBDTs	TonB-dependent transporters
TBS	Tris-buffered saline
Tris-HCl	Tris (hydroxymethyl) aminomethane hydrochloride
TSMSs	Tube-shaped membranous structures

1- Introduction

Cells are the basic unit of life, facing constant pressure from the external environment. Physical extracellular barriers, transmembrane-dependent uptake mechanisms and secretory systems are just a few examples of strategies essential for maintaining cell homeostasis (Silhavy *et al.* 2010; Sleytr *et al.* 2014; Cantine and Fournier 2018; Denise *et al.* 2020). The development of barriers external to the cytoplasmic membrane is likely among the most ancient features that cells evolved (Cavalier-Smith 2006). For example, the current classification of prokaryotic microorganisms is based on the structure of their cell envelope: the long-time, and still widely used classification of bacteria based on the Gram-staining method is due to fundamentally different cell envelope structures (Silhavy *et al.* 2010). Uptake and secretory systems are dependent on the function of membrane proteins that allow cells either to import essential nutrients or to pump out compounds from their cytoplasm, respectively (Papanikou *et al.* 2007; Krewulak and Vogel 2008; Denise *et al.* 2020). Currently, the knowledge on the composition and molecular function of these multi-protein complexes is substantial, with, for example, as many as 16 secretory systems described for bacteria only (Papanikou *et al.* 2007). However, cells can also interact with, and respond to the signals and cues originating from their extracellular medium, by membrane protein-independent systems. In this regard, the first observation of a non-classical secretion system was made on the microalga *Chlamydomonas* in the 1950s (Sager and Palade 1957; Woith *et al.* 2019), and a few years later on mammalian cells (Sotelo and Porter 1959; Woith *et al.* 2019). In these cases, cells were reported to produce vesicles, small spherical structures originating from the cells' membranes. Bacterial vesicles were described shortly thereafter in *Vibrio cholerae* and *Mycobacterium leprae* (Chatterjee *et al.* 1959; De 1959; Woith *et al.* 2019). Over the years, representatives of all major phylogenetic groups were shown to produce and release extracellular vesicles (EVs). It is therefore likely that the release of these nanosized structures (ranging between 20 and 500 nm in diameter), composed of a lipid bilayer and without the capacity of replicating, represents an ancestral bioprocess (Schwechheimer and Kuehn 2015; Coelho and Casadevall 2019; Woith *et al.* 2019; Lima *et al.* 2020; Zavan *et al.* 2020). Nevertheless, as different organisms present different cell walls/envelopes, and higher organisms can even release vesicles derived from their endomembrane system, vesicles are very heterogeneous in terms of composition (Woith *et al.* 2019). Moreover, in some instances, the same organism can even release different types of vesicles (Turnbull *et al.* 2016; Toyofuku *et al.* 2019). Despite the differences, the term "extracellular vesicles" will be used throughout this work, generally to address all kinds of vesicles released by a given organism.

EVs are now known to display crucial roles in cell homeostasis, others than the simple secretory purpose (Schwechheimer and Kuehn 2015; Joffe *et al.* 2016; Coelho and Casadevall 2019; Woith *et al.* 2019; Zavan *et al.* 2020). In bacteria, they are essential for long distance communication, nutrient uptake and virulence (Mashburn-Warren and Whiteley 2006; Kulp and Kuehn 2010; Schwechheimer and Kuehn 2015; Coelho and Casadevall 2019; Zavan *et al.* 2020). As EVs are used by microorganisms during infection, mammals have evolved strategies using those nanoparticles to stimulate their immune system (McDonald *et al.* 2014; Fais *et al.* 2016; Woith *et al.* 2019; Zavan *et al.* 2020). Furthermore, EVs in mammals are important players mediating cell communication and are increasingly studied in the frame of several pathologies *e.g.* cancer, as malignant cells can release EVs loaded with specific cancer-markers, and so, be used as a way of early diagnosis (Fais *et al.* 2016; Woith *et al.* 2019). In plants, EVs have been found to be a key defence mechanism against fungal infections, and pivotal in the symbiotic relationship with microorganisms (Mashburn-Warren and Whiteley 2006; Woith *et al.* 2019; Cui *et al.* 2020). In the latter, EVs are proposed to act in nutrient exchange and as a virulence vehicle (Joffe *et al.* 2016; Woith *et al.* 2019; Cui *et al.* 2020).

Although lipids, proteins and nucleic acids are widely found in EVs from all three domains of life (Woith *et al.* 2019), EVs from different organisms display species-specific features, such as surface structures or cargo content. For example, Gram-negative bacteria EVs are known to carry lipopolysaccharides (LPS) on their membranes, and peptidoglycan fragments in their lumen (Mashburn-Warren and Whiteley 2006; Lima *et al.* 2020; Zavan *et al.* 2020). In addition, EVs released by infectious microorganisms can carry hydrolytic enzymes, virulence factors and adhesins (Mashburn-Warren and Whiteley 2006; Kulp and Kuehn 2010; Joffe *et al.* 2016; Woith *et al.* 2019). In fact, several reports suggest that cells are capable of sorting what is packaged in EVs (Kulp and Kuehn 2010; Haurat *et al.* 2011; Lima *et al.* 2020), increasing their compositional variability and expanding their possible biological roles. As EVs' content is strongly shielded against the activity of degradative enzymes present in the environment, cargo integrity is maintained after leaving the cell and enabling its transport to distant targets, reaching longer distances than biomolecules released by the classical secretion systems (Kulp and Kuehn 2010; Lima *et al.* 2020).

The study of EVs is expanding rapidly, and it is becoming a multidisciplinary topic. Several aspects related to the composition, biological roles, biogenesis mechanisms, and even biotechnological applications of EVs are becoming increasingly investigated. The focus of the current work is on EVs released by bacteria, particularly of Cyanobacteria, a group of Gram-negative bacteria. In the following sections, details of the Gram-negative cell envelope are presented as a way of introducing relevant features

related to their EVs. Importantly, specific aspects regarding the processes of EVs formation and release in these bacteria will also be shown. As the research in cyanobacterial EVs is still lagging far behind compared to that of other Gram-negative bacteria, these initial sections will then serve as an introduction to what is known in cyanobacterial EVs and to the main objectives of this work.

1.1- The Gram-negative bacteria cell envelope

In general, the cell envelope of Gram-negative bacteria (Fig. 1) is composed of two sets of bilayered membranes (Silhavy *et al.* 2010; Goemans *et al.* 2014; Schwechheimer and Kuehn 2015; Zingl *et al.* 2020). The membrane closest to the cytoplasm is termed “inner membrane”, while the other is referred to as “outer membrane” (Silhavy *et al.* 2010; Goemans *et al.* 2014; Zingl *et al.* 2020). The inner membrane is composed of phospholipids (Kulp and Kuehn 2010; Silhavy *et al.* 2010; Zingl *et al.* 2020), while the outer membrane has an uneven composition: the internal leaflet is also composed of phospholipids, whereas the external leaflet is composed of LPS (Kulp and Kuehn 2010; Silhavy *et al.* 2010; Goemans *et al.* 2014; Schwechheimer and Kuehn 2015; Zingl *et al.* 2020). The outer membrane is responsible for the protection of the cell, and for the selectivity passage of molecules (Silhavy *et al.* 2010; Zingl *et al.* 2020). The two membranes limit a compartment known as the “periplasmic space” or “periplasm” (Kulp and Kuehn 2010; Silhavy *et al.* 2010; Goemans *et al.* 2014; Schwechheimer and Kuehn 2015). This compartment is an unusual highly oxidizing environment, and energy molecules such as ATP are absent (Kulp and Kuehn 2010; Silhavy *et al.* 2010; Schwechheimer and Kuehn 2015). Despite such extreme conditions, the periplasm harbours a great number of different molecules, and it is vital for cell survival (Silhavy *et al.* 2010). Proteins related to metal acquisition, cell envelope biogenesis and maintenance, and chaperones are examples of high abundance proteins present therein (Silhavy *et al.* 2010; Goemans *et al.* 2014). Furthermore, in the periplasm it is also possible to find the “peptidoglycan layer”, a key component of the cell envelope (Kulp and Kuehn 2010; Silhavy *et al.* 2010). This layer is composed of repeats of *N*-acetylglucosamine and *N*-acetylmuramic acid, further cross-linked with peptides (Silhavy *et al.* 2010; Zingl *et al.* 2020). The peptidoglycan is a rigid layer that dictates cell shape and resistance to high turgor pressure (Silhavy *et al.* 2010; Zingl *et al.* 2020), linking to both inner and outer membranes (Kulp and Kuehn 2010; Zingl *et al.* 2020). Those connections can be grouped in three main categories of links, namely those mediated by: lipoproteins; the outer membrane proteins (OMPs); and multi-protein complexes’ that

spawn the entire periplasmic space (Kulp and Kuehn 2010; Schwechheimer and Kuehn 2015; Zingl *et al.* 2020).

In *Escherichia coli*, the Braun's lipoprotein (Lpp) is the most abundant lipoprotein in the outer membrane (Zingl *et al.* 2020), and almost 30% of the whole Lpp pool in a cell is estimated to be linked to the peptidoglycan layer via its C-terminal region (Silhavy *et al.* 2010; Zingl *et al.* 2020). In addition, OMPs are a key component of the Gram-negative cell envelope, distinctively containing several β-barrels in their structure (Silhavy *et al.* 2010). Due to their overall high abundance, these proteins can anchor the outer membrane to the underlying peptidoglycan layer (Silhavy *et al.* 2010; Schwechheimer and Kuehn 2015; Zingl *et al.* 2020). OmpA is a major OMP from the Gram-negative cell envelope (Smith *et al.* 2007; Silhavy *et al.* 2010; Confer and Ayalew 2013; Zingl *et al.* 2020), and it has been proposed that its C-terminus binds to the diaminopimelate in the peptidoglycan layer (Park *et al.* 2012). Finally, complex systems composed of multiple protein components are capable of bridging all the three envelope layers (inner membrane-peptidoglycan-outer membrane) (Cascales *et al.* 2002; Schwechheimer and Kuehn 2015). An example of such protein complexes is the Tol/Pal system (Cascales *et al.* 2002; Zingl *et al.* 2020), which is composed of three proteins in the inner membrane, TolQ, TolR and TolA, the periplasmic component TolB, and the outer membrane lipoprotein Pal that is anchored to the membrane's inner leaflet (Zingl *et al.* 2020).

Some species of Gram-negative bacteria also display a "surface layer" (S-layer), a reticulated lattice composed by a single protein (Silhavy *et al.* 2010; Sleytr *et al.* 2014), positioned as the outermost layer of the cell envelope, linked to the outer membrane.

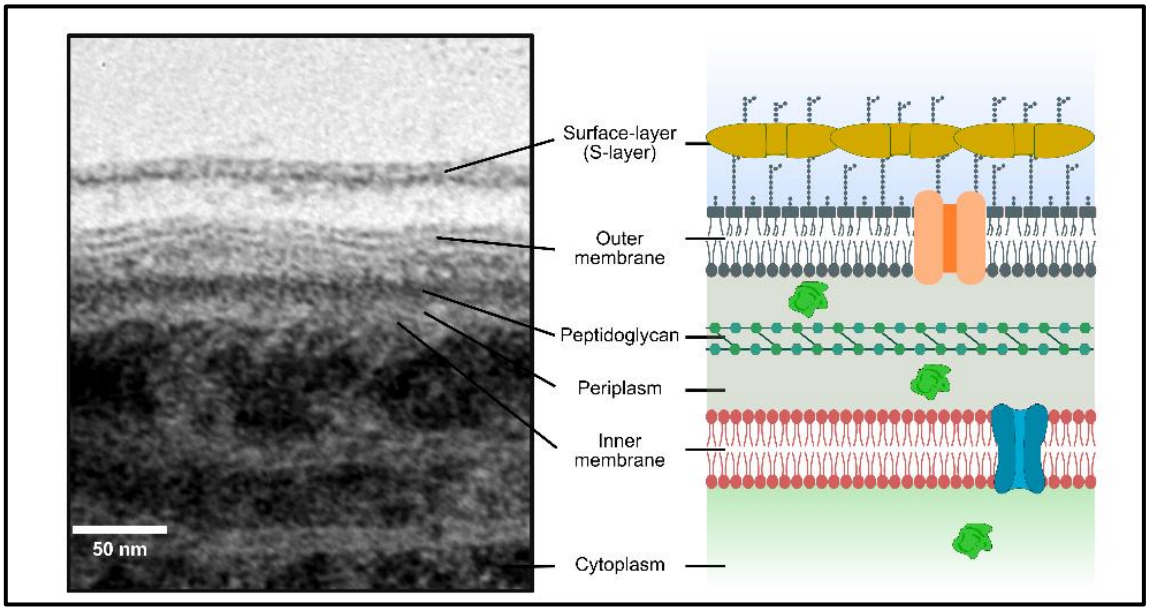


Figure 1. Ultrastructural details and model of a typical Gram-negative bacterium cell envelope.
Left panel, electron micrograph depicting details of the cell envelope of the unicellular cyanobacterium *Synechocystis* sp. PCC 6803. Right panel, schematic representation of the cell envelope (not to scale). Figure from (Lima *et al.* 2020).

1.2- Extracellular vesicles released by Gram-negative bacteria

For many years, EVs isolated from Gram-negative bacteria have been named outer membrane vesicles, as most of the evidence available pointed to the blebbing of the outer membrane as the basic mechanism underlying vesicle formation (Gonçalves *et al.* 2019; Toyofuku *et al.* 2019; Lima *et al.* 2020; Zavan *et al.* 2020). Accordingly, vesicles isolated from these bacteria contain lipids, LPS, outer membrane and periplasmic proteins, and peptidoglycan fragments (Lima *et al.* 2020; Zavan *et al.* 2020). However, nucleic acids, cytoplasmic proteins and metabolites have also been detected therein, which has raised questions as to the mechanisms of EVs formation in these bacteria (Toyofuku *et al.* 2019). Toyofuku *et al.* have recently reviewed the various types and origins of bacterial membrane vesicles, and propose a system in which they are divided in: outer membrane vesicles (OMVs); outer-inner membrane vesicles (OIMVs); explosive outer membrane vesicles (EOMVs); and tube-shaped membranous structures (TSMSs) (see Fig. 2) (Toyofuku *et al.* 2019).

The most common type of vesicles are the OMVs (Toyofuku *et al.* 2019; Lima *et al.* 2020). In this case, the vesicle is composed by a bilayered membrane limiting an aqueous lumen (Schwechheimer and Kuehn 2015). This results from the outwards blebbing of the outer membrane that eventually pinches off from the cell envelope, engulfing periplasmic content in the process (Kulp and Kuehn 2010). The OIMVs are formed as the result of a weakened linkage between the inner membrane and the

peptidoglycan layer, which allows the inner membrane to protrude into the periplasmic space, starting the vesiculation process (Toyofuku *et al.* 2019; Lima *et al.* 2020). The resulting vesicle is not only composed by the outer membrane and periplasmic space, but also includes the inner membrane and cytoplasmic content (Pérez-Cruz *et al.* 2013; Pérez-Cruz *et al.* 2015; Toyofuku *et al.* 2019; Lima *et al.* 2020). As illustrated in Fig. 2, OIMVs are distinguished from the other vesicle types by their characteristic two sets of bilayered membranes. In contrast, EOMVs and TSMSs are rather atypical vesicle types. Regarding EOMVs, they result from the "explosion" of the parental cell (Turnbull *et al.* 2016; Toyofuku *et al.* 2019; Lima *et al.* 2020), and so, the membrane fragments start to reorganize in spherical structures that entrap random molecules (Turnbull *et al.* 2016). The final result is a vesicle that contains molecules originating from all the bacterial cell structures (Turnbull *et al.* 2016; Lima *et al.* 2020). Finally, some bacterial species are able to produce unique types of membranous structures, such as nanopods, nanowires and nanotubes, which are collectively termed as TSMSs (Toyofuku *et al.* 2019; Lima *et al.* 2020; Zingl *et al.* 2020). These structures are proposed to help cells in intercellular communication, as they establish the formation of bridges between cells (Zingl *et al.* 2020), in some cases even at the periplasmic level (Toyofuku *et al.* 2019).

The different types of vesicles are likely the result of different formation routes (Toyofuku *et al.* 2019). For example, while OMVs are released by an apparent intact cell envelope, EOMVs need the parental cell to lyse, prior to their formation. The following section will briefly summarize the most well-accepted EVs formation routes, and key players involved in the biogenesis of extracellular vesicles, with special focus in OMVs, which will be referred to as EVs.

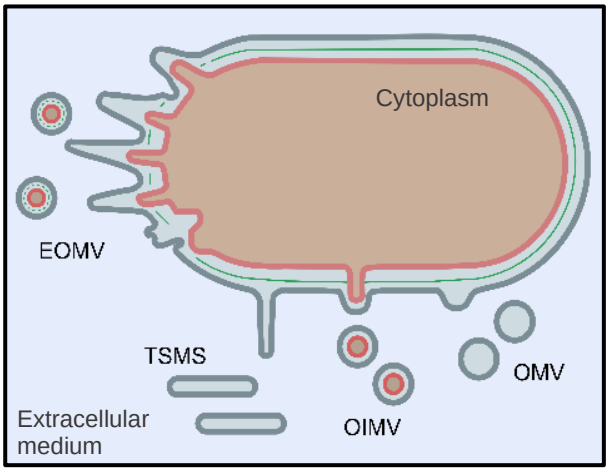


Figure 2. Types of extracellular vesicles released by Gram-negative bacteria.
Representation of a typical Gram-negative bacterium and its potential released EVs. EOMV- explosive outer membrane vesicles; TSMS- tube shaped membrane structure; OIMV- outer inner membrane vesicles; OMV- outer membrane vesicles. Figure adapted from (Lima *et al.* 2020).

1.3- Extracellular vesicles biogenesis mechanisms in Gram-negative bacteria

Vesiculation can be controlled in bacteria by shifting their specific growth conditions (Kulp and Kuehn 2010; Schwechheimer and Kuehn 2015; Zavan *et al.* 2020), either by altering physical parameters (*e.g.* temperature) (McBroom and Kuehn 2007; Kulp and Kuehn 2010; McMahon *et al.* 2012) or by supplementing the growth medium with certain compounds (*e.g.* antibiotics) (Schwechheimer and Kuehn 2015; Bauwens *et al.* 2017; Zavan *et al.* 2020; Zingl *et al.* 2020). While these adjustments in cultivation conditions allow to manipulate EVs production in a species-specific manner (McBroom and Kuehn 2007; McMahon *et al.* 2012; Schwechheimer and Kuehn 2015; Gonçalves *et al.* 2019), the underlying mechanisms that control and lead to vesiculation are less studied (Zavan *et al.* 2020). Nevertheless, three main hypotheses have been proposed to explain EVs biogenesis in Gram-negative bacteria, namely: 1) vesiculation is triggered by an alteration in outer membrane composition and properties (Toyofuku *et al.* 2019; Zavan *et al.* 2020); 2) vesiculation occurs in response to an increase of certain periplasmic components (Toyofuku *et al.* 2019; Zavan *et al.* 2020); and 3) vesiculation results from the modulation of links between the outer membrane and the remaining cell envelope constituents (Mashburn-Warren and Whiteley 2006; Toyofuku *et al.* 2019; Zavan *et al.* 2020).

As described, the outer membrane of Gram-negative bacteria is composed of phospholipids and LPS. According to the lipid microdomains EVs biogenesis hypothesis, alterations in the relative amount or on the structure of lipids and LPS may directly impact the normal vesiculation of the cell (Schwechheimer and Kuehn 2015; Toyofuku *et al.* 2019; Lima *et al.* 2020; Zingl *et al.* 2020). It has been therefore proposed that such alterations induce changes on the outer membrane fluidity and curvature, which eases the outwards bulging, and ultimately leads to EVs formation (Schwechheimer and Kuehn 2015; Lima *et al.* 2020; Zingl *et al.* 2020). To illustrate this view, it has been shown that higher amounts of lipids in the outer membrane can increase the release of EVs, and that EVs from *Porphyromonas gingivalis* are enriched in higher molecular mass LPS species (Haurat *et al.* 2011; Roier *et al.* 2016). Also, a quorum sensing molecule secreted by *Pseudomonas aeruginosa* (PQS), is known to induce high vesiculation levels not only in *P. aeruginosa* but also in other bacteria (Florez *et al.* 2017; Zingl *et al.* 2020). It has been proposed that PQS structure allows the molecule to be inserted within the outer leaflet of the outer membrane, resulting in its expansion, forming a bleb (Mashburn-Warren *et al.* 2008; Schertzer and Whiteley 2012).

Another model to describe EVs biogenesis relies in turgor pressure build-up in the periplasm (nanoterritories), which ultimately leads to outer membrane blebbing (Schwechheimer *et al.* 2014; Schwechheimer and Kuehn 2015; Lima *et al.* 2020). Accordingly, it was proposed that normally growing bacteria create turgor pressure in the periplasm as a result of debris accumulation during peptidoglycan turnover, which could cause the outer membrane to bulge (Zhou *et al.* 1998). Subsequent studies found that not only peptidoglycan fragments, but also periplasmic accumulation of proteins and LPS could induce higher vesiculation (McBroom and Kuehn 2007; Schwechheimer *et al.* 2014; Lima *et al.* 2020; Zingl *et al.* 2020), without compromising the cell envelope integrity (McBroom *et al.* 2006; Schwechheimer *et al.* 2014).

Finally, modulation of the links between the outer membrane and the remaining cell envelope components is widely accepted as a crucial step for triggering EVs formation (Mashburn-Warren and Whiteley 2006; Kulp and Kuehn 2010; Schwechheimer and Kuehn 2015; Zingl *et al.* 2020). Bacteria lacking the major OMP OmpA were shown to have an enhanced vesiculation phenotype (Song *et al.* 2008; Deatherage *et al.* 2009; Moon *et al.* 2012; Choi *et al.* 2017). These results were attributed to the reduction of the linkage pool between the outer membrane and the underlying peptidoglycan layer (Deatherage *et al.* 2009; Schwechheimer and Kuehn 2015). Accordingly, in a work in *V. cholerae* (Song *et al.* 2008), the authors found that OmpA levels inversely correlate with the number of EVs; interestingly, it was also reported that a small non-coding RNA (*vrrA*) is directly linked to the regulation of OmpA protein translation, and so, *vrrA* was described as the first sRNA to control EVs formation via modulation of OmpA levels (Song *et al.* 2008). Other outer membrane proteins can be equally important in maintaining the membrane linked to the peptidoglycan, namely lipoproteins. Mutants lacking Lpp displayed enhanced vesiculation phenotypes (Deatherage *et al.* 2009; Zingl *et al.* 2020). The fine regulation of Lpp by the cells is probably an important mechanism through which they control vesicle production (Deatherage *et al.* 2009; Schwechheimer *et al.* 2014; Schwechheimer and Kuehn 2015). Cell envelope integrity is also maintained by the Tol/Pal complex, a multi-protein system that spawns the entire periplasmic space (Cascales *et al.* 2002). This complex is responsible for connecting both membranes and the peptidoglycan layer (Zingl *et al.* 2020), and mutants in components of this complex render altered vesiculation phenotypes in different bacteria (Bernadac *et al.* 1998; Deatherage *et al.* 2009; Turner *et al.* 2015). Furthermore, the multi-protein system is known to be localized near the division site in *Salmonella typhimurium*, and deletion mutants in this system have higher vesiculation phenotypes specifically at the division site (Deatherage *et al.* 2009).

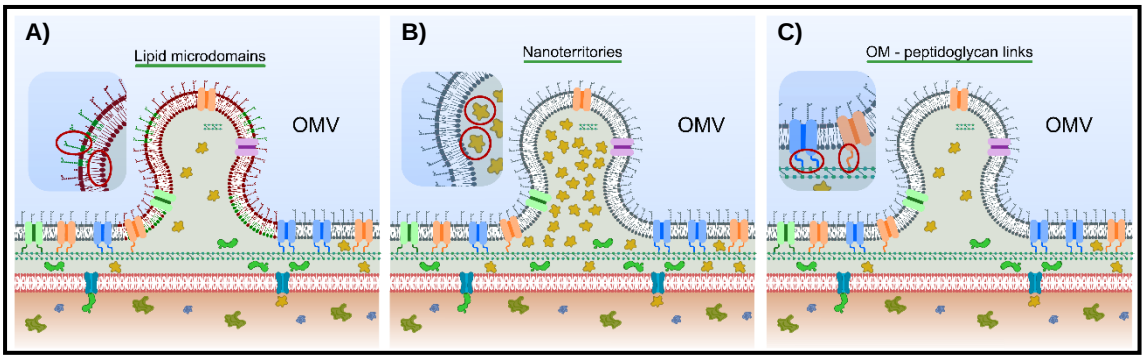


Figure 3. Mechanisms of EVs production in Gram-negative bacteria.

Panel a) EVs formation promoted by a change in the outer membrane properties induced by modification of the lipid or LPS species, and by the associated proteins. Panel b) EVs released as the result of increased turgor pressure inside the periplasmic space. Panel c) Blebbing triggered by the reduced number of links between the outer membrane and the peptidoglycan layer. Figure adapted from (Lima *et al.* 2020).

Altogether, the growing evidence in EVs biogenesis suggests that the reduction of connections between the outer membrane and the remaining components of the cell envelope represents an essential factor for vesicle formation, which is common across different biogenesis models (Mashburn-Warren and Whiteley 2006; Kulp and Kuehn 2010; Toyofuku *et al.* 2019). Likely, vesiculation in bacterial cells is triggered in multiple ways, and blebbing will occur at the "hot spots" for vesiculation, *i.e.* in the regions where the outer membrane is less linked to the other components (Mashburn-Warren and Whiteley 2006; Woith *et al.* 2019; Zingl *et al.* 2020). This does not mean that the outer membrane integrity is compromised, but it is rather loosely attached as compared with other regions.

1.4- Cyanobacteria- past and present

Cyanobacteria is a phylum of the domain bacteria known to be one of the oldest evolutionary groups, with evidence pointing to the ancestors of the group to have lived between 3.7 and 2.4 billion years ago (Sciuto and Moro 2015; Mills *et al.* 2020). The development of oxygenic photosynthesis by these organisms was a landmark in Earths' history that deeply impacted how life was going to evolve (Sciuto and Moro 2015; Mills *et al.* 2020). Cyanobacteria developed a wide range of life forms, and presently, unicellular, filamentous, and colonial forms have been described (Abed *et al.* 2009; Lau *et al.* 2015; Sciuto and Moro 2015). They can be found in a wide range of habitats, either as free-living organisms (*e.g.* benthic or planktonic in aquatic systems; soil crusts in land-based ecosystems), or in symbiosis (*e.g.* with mosses, ferns, plants) (Lau *et al.* 2015; Sciuto and Moro 2015). Some taxa are also capable to differentiate specialized cells, like heterocysts or akinetes (Lau *et al.* 2015; Sciuto and Moro 2015). On a global scale,

cyanobacteria account for 25% of Earth's primary photosynthetic productivity (Mills *et al.* 2020), corresponding to a conversion of 450 terawatts of solar energy into biomass-stored chemical energy (Yu *et al.* 2013). Furthermore, some cyanobacterial strains are also capable of fixing nitrogen (Berman-Frank *et al.* 2003; Sciuto and Moro 2015). Particularly in tropical and subtropical environments, marine cyanobacteria are estimated to fix approximately 50% of the planet's total biological combined nitrogen (Pisciotta *et al.* 2010). Recently, cyanobacteria gained a renovated biotechnological interest (Abed *et al.* 2009; Lau *et al.* 2015; Gonçalves *et al.* 2019; Mills *et al.* 2020). Several strains are already commercially available for feed and food, as they are highly rich in proteins and vitamins (Abed *et al.* 2009; Sciuto and Moro 2015; Mills *et al.* 2020). Also, and due to their intrinsic photosynthetic characteristics, these prokaryotes are considered as a green alternative for the industrial production of added value products (Abed *et al.* 2009; Yu *et al.* 2013; Lau *et al.* 2015; Gonçalves *et al.* 2019; Mills *et al.* 2020). In this regard, many cyanobacteria are natural sources of bioactive compounds (*e.g.* antibiotics), chemicals (*e.g.* pigments) and biodegradable plastics (Abed *et al.* 2009; Lau *et al.* 2015).

Cyanobacteria have long been considered Gram-negative microorganisms (Sciuto and Moro 2015). However, and as part of their own evolutionary history, these organisms developed several unique features that distinguish them from the standard Gram-negative cell envelope (Sciuto and Moro 2015). Among them, one can highlight: 1) peptidoglycan thickness and crosslinking – cyanobacteria display an unusually thick peptidoglycan layer, sometimes resembling its Gram-positive counterparts (Sciuto and Moro 2015), and it also shows different types of crosslinking, with polysaccharides linked to its chains (Hoiczyk and Hansel 2000); 2) absence of major cell envelope constituents – one of the major proteins of the Gram-negative cell envelope, the Lpp, has no known homologue in cyanobacteria (Lima *et al.* 2020); 3) outer membrane composition – it includes different features such as lipid species absent in other bacterial membranes (Lima *et al.* 2020), unusual fatty acids and even carotenoids (Hoiczyk and Hansel 2000).

Among cyanobacteria, the most well studied strain is the unicellular, non-nitrogen fixing, freshwater *Synechocystis* sp. PCC 6803 (hereafter *Synechocystis*) (Yu *et al.* 2013; Fujisawa *et al.* 2016; Mills *et al.* 2020). The genome from this model cyanobacterium was the first to be fully sequenced amid the autotrophic organisms (Kaneko *et al.* 1996; Fujisawa *et al.* 2016). However, the role of only a little more than half of the predicted coding sequences was assigned so far, and much of them by homology to other known genes in available databases (Fujisawa *et al.* 2016). Therefore, it is possible that the function of some of these predicted coding sequences has been erroneously attributed (Mills *et al.* 2020). This strongly highlights that the complete set of players involved in

several physiological, biochemical and molecular mechanisms remain to be fully described. This cyanobacterium is amenable to genetic modifications, with a wide set of molecular tools available, which have contributed towards its development as a valuable platform for metabolic engineering and synthetic biology (Yu *et al.* 2013).

1.5- Cyanobacteria- cell envelope and extracellular vesicle production

Despite the recent interest in cyanobacteria, the field of cyanobacterial EVs is just emerging (Lima *et al.* 2020). Several reports showed that distinct cyanobacterial species produce EVs, like the model cyanobacterium *Synechocystis*, but their roles and composition are still largely unknown (Xu *et al.* 2013; Pardo *et al.* 2015; Mota *et al.* 2020). An exception is the work of Biller and colleagues, in which EVs produced by the marine cyanobacterium *Prochlorococcus* were shown to be a key element in carbon fluxes in open ocean ecosystems (Biller *et al.* 2014). This was demonstrated by showing that cyanobacterial EVs were able to sustain the growth of heterotrophic bacteria in the complete absence of any other carbon source, and also by estimating the total amount of vesicles produced by these organisms to an astonishing amount of 10^{28} particles day^{-1} globally. Furthermore, EVs were also shown to be important defence mechanisms to prevent phage infection.

To date, the mechanisms underlying the formation and release of EVs in cyanobacteria are not investigated yet in detail, and only a few insights in some research articles shed some light into this topic (Oliveira *et al.* 2016; Gonçalves *et al.* 2018). In this regard, it has been shown that modifications in the cell envelope of *Synechocystis* may result in different vesiculation capacities. In particular, the presence of S-layer, a supportive but not essential external structure in the function of the cyanobacterium, which is composed by a single, very abundant and large protein, seems to represent a physical barrier for the release of EVs (Gonçalves *et al.* 2018).

Even though EVs were first regarded as cells artefacts or by-products of cellular growth, they are now recognized as crucial players in maintaining cell homeostasis as well as in mediating inter-kingdom communication (Coelho and Casadevall 2019; Cui *et al.* 2020; Zavan *et al.* 2020). In this respect, the lack of research on EVs secreted by cyanobacteria limits our understanding of their pivotal roles in the environment, as initially demonstrated by Biller *et al.* (Biller *et al.* 2014). Moreover, cyanobacteria are becoming increasingly accepted as green alternatives for biotechnological applications, and the development of strategies applying EVs (*e.g.* as platforms for vaccines), can further increase the interest and utility of these microorganisms.

1.6- Objectives

The current knowledge of the cyanobacterial cell envelope composition and formation mechanisms points to the existence of several differences as compared to other Gram-negative bacteria. In this regard, the question of whether the proposed mechanisms for EVs biogenesis hold true for cyanobacteria arises. Therefore, the main goal of this work was **to validate some of the described biogenesis mechanisms proposed for EVs formation in Gram-negative bacteria in the model cyanobacterium *Synechocystis***. To that end, two approaches were followed:

1) To investigate the modifications occurring at the cyanobacterial cell envelope and on the production of EVs, resulting from the deletion of genes encoding outer membrane proteins possibly linking the outer membrane to the underlying peptidoglycan layer;

2) To study the release and cargo composition of EVs isolated from cyanobacterial strains with increased periplasmic pressure resulting from the accumulation of heterologous proteins.

2- Material and Methods

2.1- Organisms and culture medium

2.1.1- Cyanobacterial cultivation and maintenance conditions

The unicellular, non-nitrogen fixing cyanobacterium *Synechocystis sp*. PCC 6803 was grown in standard liquid BG11 medium (Stanier *et al.* 1971), using 100 mL Erlenmeyer flasks, at 28 ºC in a 16 h light (15 µmol photons m^{-2} s^{-1}) / 8 h dark cycles regime, with constant agitation (70 rpm, OVAN). Mutant strains (Table 1) were maintained in BG11 medium supplemented with 100 µg mL^{-1} kanamycin. Cyanobacterial strains were routinely streaked onto solid BG11 supplemented with 4.79 g L^{-1} of sodium thiosulfate pentahydrate and 1% (w/v) Noble agar (Difco) to confirm the axenic state of the cultures. Culture growth was monitored by measuring optical density using the spectrophotometer UVmini-1240 (Shimadzu) at 730 nm (OD_{730}).

In general, for experimental analyses (see specific details below), cyanobacterial cultures grown in BG11 medium (supplemented with antibiotics, when necessary) for one week in Erlenmeyer flasks were used to inoculate 200 mL cultures of an initial OD_{730} of 0.05. Cultivation, without antibiotics, was performed in glass gas washing bottles with aeration (approx. 1 L air min^{-1}) in a 16 h light (30 µmol photons m^{-2} s^{-1}) / 8 h dark cycle, until a final OD_{730} of 0.8 - 1.2.

Table 1. ***Synechocystis*** **sp. PCC 6803 mutant strains used in this work.**

Mutant strain	Genotype
Δ1908	Deletion of *slr1908* by insertion of the KmR[1] cassette
Δ0042	Deletion of *slr0042* by insertion of the KmR cassette
Δ1550	Deletion of *sll1550* by insertion of the KmR cassette
Δ0772	Deletion of *sll0772* by insertion of the KmR cassette
Δ1271	Deletion of *sll1271* by insertion of the KmR cassette
L::noSP	Insertion of the construct $P_{trc.X.lacO}$::sfGFP in the neutral site 15
L::Fut	Insertion of the construct $P_{trc.X.lacO}$::*futA2* SP[2]::sfGFP[3] in the neutral site 15
R::noSP	Insertion of the construct P_{rbcL}::sfGFP in the neutral site 15
R::Fut	Insertion of the construct P_{rbcL}::*futA2* SP::sfGFP in the neutral site 15

[1] KmR – kanamycin resistance cassette obtained from plasmid pUC4K

[2] SP – signal peptide

[3] sfGFP – superfolder-green fluorescent protein

2.1.2- *Escherichia coli*

E. coli strain XL1 Blue was routinely used for intermediate steps in plasmid construction. Individual colonies were grown overnight in liquid medium, in standard LB medium and with agitation (150 rpm), or in LB solid medium, supplemented with 1.5 % (w/v) agar. When necessary, medium was supplemented with antibiotics (100 μg mL^{-1} ampicillin or 50 μg mL^{-1} kanamycin).

2.2- Plasmid Construction and mutant generation

To generate knockout mutants of the genes encoding outer membrane porins in *Synechocystis*, a classical double homologous recombination approach was taken. To that end, one plasmid was generated for each gene of interest. For details of each step, please check sections below.

The recombination platforms (approximately 600 bp) for each gene knockout were amplified by PCR using specific oligonucleotides (see Table 2) and using genomic DNA isolated from *Synechocystis* as template. As the oligonucleotides' sequences were designed to harbour recognition sites for various restriction enzymes, the DNA fragment corresponding to the 5' recombination platform was digested with XhoI and PstI, while the 3' recombination platform was digested with PstI and BamHI, following the manufacturer's instructions (Thermo Fisher Scientific). In addition, plasmid pBluescript SKII (+) was digested with XhoI and BamHI. Assembly of the 3 digested DNA fragments was performed by ligation with T4 DNA ligase (Thermo Fisher Scientific), and later transformed into *E. coli* chemically competent cells. Transformed single colonies were inoculated in liquid LB medium, and the respective plasmids were isolated using the NZYMiniprep kit (NZYTech), following the manufacturer instructions. Identity of the successfully assembled plasmids was determined by Sanger sequencing (StabVida), resulting in plasmids pDC1841, pDC1908, pDC0042, pDC1550, pDC0772, and pDC1271. Later, the kanamycin resistance cassette from the plasmid pUC4K (GE Healthcare) was amplified using specific oligonucleotides (Table 2). The resulting DNA fragment was digested with PstI, as well as each of the generated plasmids. DNA fragments were assembled by ligation and transformed into *E. coli*. Kanamycin resistant colonies were selected for plasmid isolation, and the resulting plasmids were named pDC1841K, pDC1908K, pDC0042K, pDC1550K, pDC0772K, and pDC1271K. Constructed plasmids were used to transform *Synechocystis*, and fully segregated mutant strains Δ*1908*, Δ*0042*, Δ*1550*, Δ*0772*, Δ*1271* were obtained.

2.2.1- DNA extraction from *Synechocystis* cultures

For DNA extraction, the well-established protocol by (Tamagnini *et al.* 1997) was used. Ten mL of culture were harvested by centrifugation at room temperature for 10 min at 4400 *g* (Hettich® Universal 320R). The supernatant was discarded and the cells were washed twice in 5 mL of resuspension buffer (50 mM Tris-HCl, 5 mM EDTA, pH 8.0), and centrifuged at 4400 *g* for 5 min. Cell pellet was then suspended in 500 µL of resuspension buffer, and the mixture transferred to a 2 mL screw-cap tube containing 250 µL chloroform, 250 µL phenol, 25 µL of 10% (w/v) SDS and 0.35 g of acid-washed glass beads (0.6 µm diameter). Next, sample was vigorously vortexed in 5 cycles of 30 sec each, and resting 1 min on ice between vortexing cycles, followed by a 10 min centrifugation at 16100 *g*, at 4 ºC (Eppendorf® Microcentrifuge 5415R) for phase separation. The aqueous phase was transferred to a new 2 mL tube, mixed with 500 µL of chloroform, vortexed for 5 sec, and centrifuged for 5 min at 16100 *g*, at 4 ºC. The aqueous phase was transferred to a new 1.5 mL microfuge tube, and DNA was precipitated with 3 M sodium acetate (pH 5.2) and ice-cold, absolute ethanol, at -20 ºC for approximately 2 h. The sample was then centrifuged for 20 min at 14000 *g*, at 4 ºC. The resulting pellet was washed with 1 mL of 70% (v/v) ice-cold ethanol and centrifuged for 10 min at 14000 *g*, at 4 ºC. The supernatant was carefully discarded, and the DNA was left to dry for 1 h on ice. Finally, the DNA was suspended in 50 µL of water, quantified on a Nanodrop 1000, and stored at -20 ºC until further analysis.

2.2.2- Polymerase chain reaction (PCR)

For polymerase chain reactions, Phusion High-Fidelity DNA Polymerase (Thermo Scientific) was the enzyme of choice to amplify DNA fragments for subsequent cloning, while for routine DNA amplification (*e.g.* assessment of chromosome segregation), GoTaq® Flexi DNA Polymerase (Promega) was used. All enzymatic reactions were carried following the manufacturers' instructions for a final volume of 20 µL with 0.2 mM of dNTPs. For reactions using Phusion High-Fidelity DNA Polymerase the reaction mix was composed of 0.02 U of enzyme and 0.5 µM of each oligonucleotide. When using the GoTaq Flexi DNA Polymerase, the reaction mix contained 0.025 U of enzyme and 1 µM of each oligonucleotide. For colony PCRs, *Synechocystis* cells were collected from agar plates and suspended in 10 µL of BG11. Two µL of cell suspension were then used instead of isolated DNA.

Table 2. Oligonucleotides used in this work.

Primer	Purpose	Sequence	Product size (bp)	Restriction Enzyme	T_a (ºC)
slr1841 5'F	slr1841 5' recombination plaform	Aaa**ctcgag**agtccctgttagtgagccct	651	XhoI	63
slr1841 5'R		Aaactgcagcgagacgagtgaccaacagg		PstI	
slr1841 3'F	slr1841 3' recombination plaftorm	Aaactgcagtgggttacttggctagcacg	663	PstI	63
slr1841 3'R		Aaa*ggatcc*gcagagggttagcagtggtt		BamHI	
slr1908 5'F	slr1908 5' recombination platform	Aaa**ctcgag**agtccacaggtgaattggcc	580	XhoI	63
slr1908 5'R		Aaactgcaggcgccgaagttgtcaatgtt		PstI	
slr1908 3'F	slr1908 3' recombination platform	Aaactgcagctggattggcggtactggtt	668	PstI	63
slr1908 3'R		Aaa*ggatcc*agggcatcaaaccaccactc		BamHI	
slr0042 5'F	slr0042 5' recombination platform	Aaa**ctcgag**gtgacatcggtttcggagtt	647	XhoI	63
slr0042 5'R		Aaactgcagggttggagattttggggatt		PstI	
slr0042 3'F	slr0042 3' recombination platform	Aaactgcaggcctaacgatgtggtcgatt	629	BamHI	63
slr0042 3'R		Aaa*ggatcc*tagagtcgccttccggatta		PstI	
sll1550 5'F	sll1550 5' recombination platform	Aaa**ctcgag**gggacagatcacttccgtgt	566	XhoI	63
sll1550 5'R		Aaactgcagacactggctggaaagtaccg		PstI	
sll1550 3'F	sll1550 3' recombination platform	Aaactgcagacccgtagcccgatctattt	581	PstI	63
sll1550 3'R		Aaa*ggatcc*tcaatgtcagtggtggcaat		BamHI	
sll0772 5'F	sll0772 5' recombination platform	Aaa**ctcgag**ggcaatggcgttaatcaagt	689	XhoI	63
sll0772 5'R		Aaactgcagacagtacccaagcgcagagt		PstI	
sll0772 3'F	sll0772 3' recombination platform	Aaactgcagagctggctttaattggcaga	636	PstI	63
sll0772 3'R		Aaa*ggatcc*ttaagcacgacccaaaaacc		BamHI	
sll1271 5'F	sll1271 5' recombination platform	Aaa**ctcgag**aacgacaatgccaaaacctc	648	XhoI	63
sll1271 5'R		Aaactgcaggcggcaaagttaaaatcag		PstI	
sll1271 3'F	sll1271 3' recombination platform	Aaactgcagatcgcccccatttatttacc	574	PstI	63
sll1271 3'R		Aaa*ggatcc*cggtggtagcgggagtaata		BamHI	
pUC 4K F	kanamycin resistance cassette	aaactgcagtgaggtctgcctcgtgaagaa	1226	PstI	64
pUC 4K R		aaactgcagaaagccacgttgtgtctcaaa		PstI	

The pair of oligonucleotide used for the amplification of the kanamycin resistance cassette was taken from (Oliveira *et al.* 2016). All the remaining oligonucleotides were designed and synthesized for this work.

2.2.3- Agarose gel electrophoresis

All DNA samples' analyses were performed in 0.8% (w/v) agarose (NZYTech) gels prepared in TAE buffer (40 mM Tris, 20 mM acetic acid, 1 mM EDTA, pH 8.3). Electrophoresis was carried at 150 V in the PowerPac™ Basic (Bio-Rad), and DNA staining was performed with GreenSafe Premium (NZYTech). DNA was visualized by exposure to UV light in a Gel-Doc system (Bio-Rad). When necessary, DNA fragments were isolated with the Gel Pure kit (NZYTech), as described by the manufacturer.

2.2.4- DNA ligation reactions

DNA ligation was performed overnight at 22 ºC using the T4 DNA Ligase (Thermo Fisher Scientific). For the reaction mixture, 2.5 U of enzyme was added to a 1:3:3 DNA ratio of vector to recombination platforms. For the ligation of a vector to the kanamycin resistance cassette, 1:3 ratio (vector:insert) was applied. Reactions were inactivated at 65 ºC for 15 min prior to transformation.

2.2.5- *E. coli* transformation

For *E. coli* transformation, 7 µL of inactivated DNA ligation, or 1 µL of isolated plasmid, were added to 100 µL of *E. coli* XL1 Blue competent cells followed by an incubation on ice for 30 min with gentle agitation. After the incubation, a heat shock was performed at 42 ºC for 45 sec, followed by a 2 min incubation on ice. Subsequently, 900 µL of pre-heated LB medium was added, and the cells agitated at 150 rpm for 1 h at 37 ºC. Next, cells were placed on solid LB medium supplemented with the proper antibiotic (100 µg mL^{-1} ampicillin or 50 µg mL^{-1} kanamycin), and further incubated at 37 ºC overnight.

2.2.6- *Synechocystis* transformation

For the natural transformation of *Synechocystis* the method described by (Heidorn *et al.* 2011) was followed. A 50 mL culture was inoculated at an initial OD_{730} of 0.1 in 100 mL Erlenmeyer flasks. When the culture reached an OD_{730} of 0.5, 10 mL were harvested and centrifuged at room temperature for 10 min at 4400 *g*. The cell pellet was suspended in sterile BG11 medium to a final OD_{730} of 2.60. Next, 500 µL of cyanobacterial culture were mixed with 10 µg of the plasmid of interest, and the mixture was incubated for 6 h at 30 ºC, under an irradiance of 20 µmol photons m^{-2} s^{-1}, and with agitation. Then, cells were transferred to solid BG11 medium without antibiotic, and incubated for 24 h at 30 ºC under constant light (20 µmol photons m^{-2} s^{-1}). Cells were transferred to solid BG11 medium containing 15 µg mL^{-1} kanamycin and incubated at 30 ºC under a constant irradiance of 20 µmol photons m^{-2} s^{-1}. Transformed colonies appeared approximately 1-2 weeks after transformation. Transformed *Synechocystis* colonies were then periodically transferred to fresh solid BG11 medium plates supplemented with an increasing antibiotic concentration, following the scheme 15, 50 and 100 µg mL^{-1} kanamycin. After reaching the highest kanamycin concentration, transformants were weekly screened to evaluate chromosome full segregation by using colony PCR, which was repeated at least twice in consecutive weeks. Colonies corresponding to fully segregated mutants were transferred to liquid BG11 medium

containing 100 µg mL^{-1} kanamycin and cultivated under standard growth conditions. Finally, prior to mutant characterization, an additional chromosome segregation test was performed by PCR using isolated genomic DNA as template (see 2.2.2- DNA extraction from *Synechocystis* cultures).

2.3- Characterization of *Synechocystis* mutants

2.3.1- Growth rates

To evaluate the growth capacity of each *Synechocystis* mutant strain used in this work (Table 1), cultivation experiments in liquid BG11 medium were carried out in 96-well clear bottomed microplates at 30 ºC with a 16 h light (50 µmol photons m^{-2} s^{-1})/ 8 h dark cycle with agitation (150 rpm), unless stated otherwise. Prior to each experiment, cyanobacterial cultures were inoculated in 100 mL Erlenmeyer flasks at an initial OD_{730} of 0.5, supplemented with kanamycin when necessary, and cultivated as described above (2.1.1- Cyanobacterial cultivation and maintenance conditions) for 7days up to an OD_{730} of 1.0-1.8. Cultures were diluted to an OD_{730} of 0.4, and distributed onto the microplates in technical triplicates. On a daily basis, cells were suspended by pipetting, and optical density at OD_{730} was monitored on a microplate reader (Synergy Mx, BioTek).

In the particular case of the *Synechocystis* single-deletion mutants lacking outer membrane proteins, growth was also monitored in modified liquid BG11 medium, in which iron ammonium citrate was either absent, or supplied in 2-fold amount, as compared to standard BG11 medium. Moreover, three cultivation setups were tested, including: 1) cells cultivated in constant light; 2) cells cultivated in light/ dark cycles (16 h light/ 8 h dark); or 3) cells pre-adapted for one week in modified BG11 medium lacking iron ammonium citrate (major iron source in BG11 medium) in Erlenmeyer flasks, and then grown in a 16 h light/ 8 h dark cycle regimen. Irrespective of the tested condition, *Synechocystis* strains were washed three times in modified BG11 medium lacking iron ammonium citrate prior to being distributed onto the microtiter plates.

2.3.2- Outer membrane isolation and purification

As described above (2.1.1- Cyanobacterial cultivation and maintenance conditions), pre-cultures were inoculated in 100 mL Erlenmeyer flasks for one week, and then used as inoculum for 200 mL cultures in glass gas washing bottles. Cells were pelleted at 4400 *g* for 10 min at room temperature and the pellet corresponding to 50 mL of grown culture was washed in 1 mL of buffer O (10 mM Tris-HCl, pH 7.45). The mixture was then transferred to a 1.5 mL microfuge tube and centrifuged at 16100 *g* for 2 min at 4 ºC. Cells were suspended in 400 µL of buffer O and lysed by sonication (Branson

Sonifier 250 (output 3-4, 50% duty cycle)) in 5 cycles of 15 sec power, 15 sec on ice. Then, cell lysates were centrifuged for 15 sec at 16100 *g* (4 ºC) to remove unbroken cells and heavy cellular debris, and the supernatant was further centrifuged for 30 min at 16100 *g* (4 ºC). The resulting pellet was washed in 200 µL of buffer O, and centrifuged once again for 30 min under the same conditions. Next, the pellet was suspended in 200 µL buffer O, and mixed with 250 µL of buffer O containing 2% (v/v) N-Lauroylsarcosine. The mixture was incubated for 30 min with agitation in the Roto-Torque (Cole-Parmer) at room temperature. Outer membranes were then collected by centrifugation (45 min at 16100 *g* (4 ºC)), and washed twice in 400 µL of buffer O. In the end, isolated outer membranes were suspended in 50 µL of buffer O and stored at -20 ºC.

2.3.3- Extracellular medium isolation and concentration

To study the cyanobacterial growth medium after cell cultivation, *Synechocystis* wild-type and mutant strains were cultivated as described above (2.1.1- Cyanobacterial cultivation and maintenance conditions). Biomass was collected by centrifugation at room temperature for 10 min at 4400 *g*, and the remaining cells were further removed from the growth medium by filtration using either 0.2 µm or 0.45 µm size filters (Fisher Scientific). Then, cell-free extracellular medium was concentrated to a final volume of approximately 200 µL by ultrafiltration using the Amicon® Ultra-15 Centrifugal Filters (3 kDa molecular weight cut-off, Merck) by centrifugation at 4400 *g* (16 ºC). Concentrated samples were stored at -20 ºC until further analysis.

2.3.4- Isolation and characterization of extracellular vesicles

To isolate EVs produced by *Synechocystis* wild-type and mutant strains, cells were previously cultivated in 200 mL glass gas washing bottles (initial OD_{730} of 0.05), grown for 3.5 days, and later used to inoculate 600 mL cultures in 1 L glass gas washing bottles (initial OD_{730} of 0.05). Cells were then cultivated for 4 days in the same growth conditions up to a final OD_{730} of approximately 1.0. After cultivation of the various cyanobacterial strains, cells were pelleted by centrifugation for 15 min at 3836 *g* (High speed Centrifuge Beckman Avanti J-26 XP, Beckman Coulter Life Sciences). The extracellular medium was further filtered through 0.45 µm size filters to ensure complete cell removal, and later concentrated to 15 mL in Macrosep® Advance Centrifugal Devices (100 kDa molecular weight cut-off, Pall). Samples were then ultracentrifuged at 100000 *g* for 3 h at 4 ºC. The vesicle pellet was suspended in approximately 200 µL of extracellular medium, and stored at -80 ºC until further analysis.

2.3.4.1- Transmission electron microscopy

For observation of EVs samples by transmission electron microscopy, the negative-staining method was used as described (Oliveira *et al.* 2016). Ten µL samples were mounted on formvar/carbon film coated mesh nickel grids (Electron Microscopy Sciences) and liquid in excess was removed with filter paper after 2 min. Then, 5 µL of 1% (w/v) uranyl acetate were loaded on the grids for 10 sec, and the excess removed with filter paper. Prepared samples were visualized in a Jeol JEM-1400 transmission electron microscope, operating at 80 kV.

2.3.4.2- Nanosight

To characterize the extracellular vesicles samples' concentration and size distribution, isolated vesicle fractions were analysed by nanoparticle tracking analysis using the NanoSight NS300 NTA Dev Build 3.2.16 (Malvern), equipped with an sCMOS camera. Samples were diluted in filtered PBS solution (between 1:1000 and 1:10000 (137 mM NaCl, 2,7 mM KCl, 10 mM NA_2HPO_4, 1.8 mM KH_2PO_4, pH 7.5)), and further analyzed as described (Oliveira et al., 2016). In brief, three movies of 30 s were recorded for each sample (with a threshold of 10 to 50 particles per frame), with the following capturing settings: camera level 14-16, slider shutter 1300, slider gain 512, at 23 ºC, and with a syringe pump speed of 40. Data acquisition and processing were performed using the NanoSight NS300 NTA 3.0 software, using a detection threshold of 5.

2.3.4.3- Lipopolysaccharide staining

For detection of the outer membrane structural component LPS, concentrated extracellular medium samples were heat-denatured with Laemmli buffer at 95 ºC for 10 min, and further incubated with 0.2 U of protease type XIV from *Streptomyces griseus* (Sigma-Aldrich), for 30 min at 37 ºC. Samples were then loaded in 16% (w/v) SDS-polyacrylamide gels and LPS were separated by electrophoresis. Later, staining was performed using the Pro-Q™ Emerald 300 Lipopolysaccharide Gel Stain Kit (Thermo Fisher Scientific), following the manufacturer's instructions. Visualisation and image acquisition was carried out with exposure to UV light in the Gel-Doc system. For quantification of relative LPS abundance, densitometry analysis was carried out using the ImageJ software (Schneider *et al.* 2012).

2.3.5- Protein analysis and Western blotting

To study the protein composition of isolated outer membrane preparations, samples were heat-denatured for 10 min at 95 ºC in solubilization buffer (5% (v/v) 2-mercaptoethanol, 0.025% (w/v) bromophenol blue, 10% (w/v) glycerol, 2% (w/v) SDS, 62.5 mM Tris-HCl pH 6.8), and separated by electrophoresis in 12% (w/v) SDS-polyacrylamide gel.

For extracellular protein analysis, concentrated extracellular medium samples were first heat-denatured for 10 min at 95 ºC with Laemmli buffer (1.25% (v/v) 2-mercaptoethanol, 10% (v/v) glycerol, 0.5% (w/v) SDS, 0.025% (w/v) bromophenol blue in 125 mM Tris-HCl pH 6.8). Proteins were separated by electrophoresis on 4-15% (w/v) SDS–polyacrylamide gels (Bio-Rad). All samples were first normalized for the culture final OD_{730}, volume of extracellular medium to be concentrated (mL) and concentration factor.

After electrophoresis, gels were incubated for 1 h in fixing solution (7% acetic acid and 40% methanol), and then stained over-night with PageBlue™ Protein Staining Solution (Thermo Fisher Scientific) with continuous agitation, following the manufacturer instructions. For image acquisition, gels were washed several times in distilled and deionized water, and scanned with the GS-800 Calibrated Densitometer (Bio-Rad).

For protein identification, outer membrane protein and exoproteome samples were separated in 10% or 12% (w/v) SDS-polyacrylamide gels, respectively. Bands of interest were cut out from the gel, in-gel digested with trypsin, and analysed by LC-MS system comprehending a nanoUHPLC on-line coupled to a high-resolution accurate-mass Orbitrap mass spectrometer (Q Exactive, Thermo Scientific).

To detect the amount of sfGFP in the extracellular media and, particularly, isolated EVs, Western-blot analyses were performed with an antibody that specifically recognizes sfGFP. For that, samples were loaded in a 16% (w/v) SDS–polyacrylamide gel and further separated by electrophoresis. After protein separation, the gel was incubated for 15 min in 25 mL of transfer solution (48mM Tris-HCl pH 8.3, 39 mM glycine, 0.04% (w/v) SDS, 20% (v/v) methanol), at room temperature with agitation (70 rpm). The nitrocellulose membranes were previously activated on water for 10 sec, and then incubated in 25 mL of transfer solution for 15 min. Protein transfer was carried out in the Trans-blot® semi-dry electrophoretic transfer cell for 80 min. Later, membranes were rinsed twice in 20 mL Blocking solution [5% (w/v) fat-free milk powder, 1x TTBS (0.05% (v/v) Tween-20, 1x TBS (0.14 M NaCl, 20 mM Tris-HCl pH 7.6))], followed by a minimum period of 1 h incubation in 25 mL of blocking solution with agitation, and incubated over-night at 4 ºC in 15 mL of fresh blocking solution with primary antibody (1:5000, monoclonal mouse anti-GFP antibody, Roche®). Then, membranes were rinsed twice in

20 mL of TTBS, and further washed for three times with 50 mL of TTBS for 15 min at maximum agitation. Secondary antibody (goat Anti-mouse IgG, Santa Cruz Biotechnology) incubation was performed for 80 min to a final concentration of 1:5000 in 15 mL of fresh blocking solution. Membranes were washed 3 times with TTBS, and twice with TBS. Finally, blots were developed with Clarity Western ECL Substrate (Bio-Rad) following the manufacturer's instruction, and image acquisition was obtained using the Chemidoc system (Bio-Rad).

2.3.6- Fluorescence measurements

To evaluate the amount of fluorescence signal emitted by the mutant strains harbouring the sfGFP constructs, cells were grown in liquid BG11 medium in 96-well clear bottomed microplates, as described above (2.3.1- Growth rates). Prior to each experiment, cell cultures were washed with sterile BG11 medium. Fluorescence measurements were monitored daily on the microplate reader (Synergy Mx, BioTek), by collecting emitted light at 528 nm (20 nm band gap) when samples were excited at 488 nm (9 nm band gap). The dynamics of the total and intracellular fluorescence were measured for the first four days of growth. For that, four microplates were simultaneously prepared, each representing one time-point. Every day, 1.2 mL of each culture were transferred from the cultivation plate to a 1.5 mL microfuge tube, and 200 µL of the cell suspension were used to measure the culture's OD_{730} and total fluorescence signal. The remaining culture was centrifuged for 10 min at 4000 *g*, and the collected cells were suspended in the same volume of fresh, sterile BG11 medium; the fluorescence signal detected from this sample was regarded as corresponding to that emitted by the sfGFP present in cells only (intracellular fluorescence). Optical density and fluorescence measurements were performed as described, on 96-well microtiter plates. Fluorescence levels for all tested strains were normalized by the corresponding amount of cells in the sample, as determined by optical density (OD_{730}).

2.3.7- Statistical analysis

Statistical analyses were performed with one-way ANOVA using the Analysis ToolPak-VBA supplement available for the Microsoft Office Excel (Microsoft).

3- Results and Discussion

The main goal of this project was to study extracellular vesicles biogenesis mechanisms in cyanobacteria. From the hypothesized routes described in well-characterized model Gram-negative bacteria for EVs formation, two were selected: 1) modulation of outer membrane-peptidoglycan layer links; and 2) nanoterritories resulting from increased periplasmic pressure. In the following sections the obtained results will be presented and discussed in light of current literature.

3.1- Modulation of Outer Membrane-Peptidoglycan layer links

3.1.1- Identification of candidate proteins and generation of mutant strains

To study the effects of reducing the overall linkage capacity between the outer membrane and the underlying peptidoglycan layer on the production of EVs in cyanobacteria, the first step was to identify candidate proteins that could potentially bridge both layers. In the model bacterium *E. coli*, Lpp and OmpA family proteins fulfil that role (Silhavy *et al.* 2010; Lima *et al.* 2020; Zingl *et al.* 2020). An *in-silico* analysis of the model cyanobacterium *Synechocystis* showed that no homologues of the lipoprotein Lpp can be found (Lima *et al.* 2020); in contrast, 6 genes encoding putative outer membrane proteins, homologous to the OmpA protein family could be identified (Oliveira *et al.*, unpublished), corresponding to genes: *slr1908*, *slr1841*, *sll1271, sll0772*, *slr0042*, and *sll1550* (Fig. 4A). Despite the homology to OmpA protein family members, the predicted *Synechocystis* proteins harbour two distinctive, and conserved protein domains: the S-layer homology domain (SLH), and the carbohydrate-selective porin OprB (OprB) (Fig. 4B). The SLH domain was first characterized in Gram-positive bacteria, shown to interact non-covalently with the S-layer (Mesnage *et al.* 2000). Later, it was found that several cyanobacterial OMPs contain this domain (Hoiczyk and Hansel 2000; Kojima *et al.* 2016). Kojima *et al*. demonstrated that the SLH-domain, particularly that found in proteins Slr1841, Slr1908 and Slr0042 bind the peptidoglycan layer (Kojima *et al.* 2016). In its turn, the OprB domain was first described in *P. aeruginosa*, reported to form a pore-like structure in the outer membrane of this Gram-negative bacterium, being responsible for glucose uptake (Trias *et al.* 1988). To check for the presence of proteins containing SLH-OprB-domains in the outer membrane, outer membrane protein preparations from *Synechocystis* were isolated and separated by electrophoresis on SDS-polyacrylamide gels. Identification of the most abundant proteins detected in the outer membrane samples further showed that proteins containing SLH-OprB-domains (Slr1841 and Slr1908) are present in high abundance (Fig. 4C). Altogether, these results suggest that cyanobacterial proteins harbouring these two domains may play a structural role in the cell envelope, by anchoring the outer membrane to the peptidoglycan layer,

as well as mediating the import of specific nutrients, in agreement with earlier suggestions by (Kowata *et al.* 2017; Qiu *et al.* 2018).

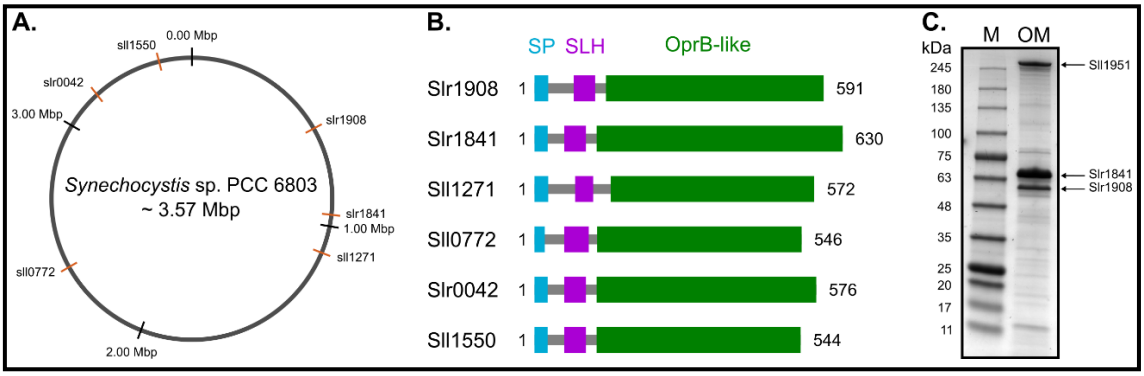


Figure 4. *Synechocystis* sp. PCC 6803 outer membrane proteins homologous to the OmpA protein family and their coding genes.

A. Schematic representation of the *Synechocystis* genome, and relative position of each gene encoding putative outer membrane proteins homologous to the OmpA protein family. **B.** Details of the size (in amino acids), and relative position of signal peptide (SP) and conserved domains (SLH – S-layer homology; OprB –carbohydrate-selective porin OprB domain) in the identified putative outer membrane proteins. **C.** PageBlue™ (Thermo Fisher Scientific) stained 4-15% (w/v) SDS-polyacrylamide gel showing the protein composition of isolated *Synechocystis* outer membrane preparations. Highlighted protein bands were identified by mass spectrometry.

In order to evaluate the role played by these proteins, single knockout mutants of the respective genes were generated. For the partial deletion of each gene of interest by double homologous recombination, six plasmids were constructed (see 2.2- Plasmid Construction and mutant generation): pDC1841K, pDC1908K, pDC0042K, pDC1550K, pDC0772K, and pDC1271K. In Fig. 5, the scheme of one of the plasmids constructed in this work is represented.

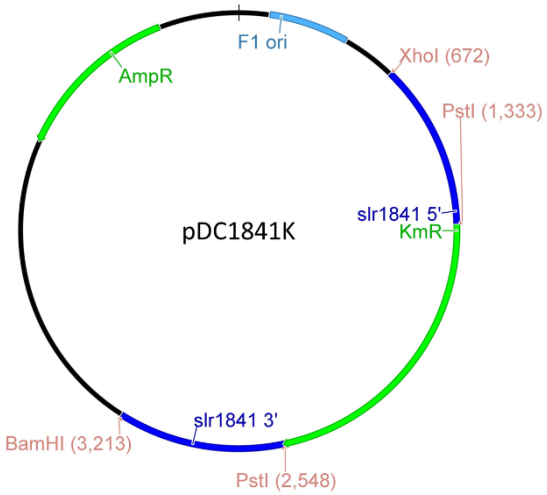


Figure 5. Representation of the pDC1841K plasmid used in this work.

Each of the six plasmids generated contain the same basic features: AmpR- ampicillin resistance cassette; F1 ori- plasmid origin of replication. Furthermore, each plasmid contains two recombination platforms: 5' platform between the XhoI and PstI restriction sites, and 3' platform between the BamHI and PstI recognition sites. Both elements are represented in blue. KmR- kanamycin resistance cassette, inserted between the recombination platforms.

The generated plasmids were introduced into *Synechocystis* cells by natural transformation, and segregation was verified by PCR using the oligonucleotides comprising the 5' F and 3' R of each gene in the respective mutant (Fig. 6).

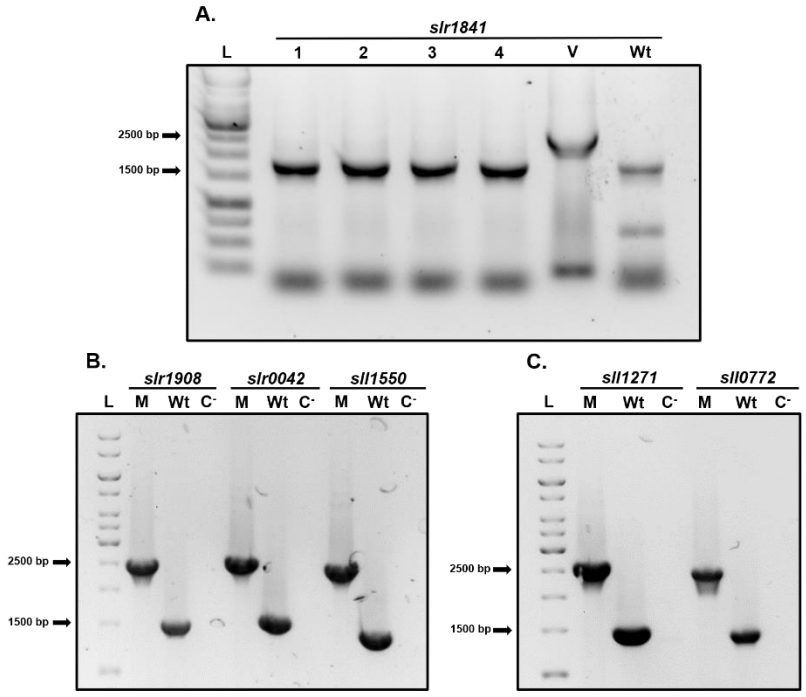


Figure 6. Chromosome segregation analysis of the genes encoding proteins containing SLH-OprB-domains.
A. Green-safe stained agarose gel showing the result of a *Synechocystis* colony PCR using specific oligonucleotides (5' F and 3' R) for the *slr1841* gene in transformants grown for one week in solid BG11 medium supplemented with 200 µg mL^{-1} kanamycin (1 to 4). Vector pDC1841K (V), and wild-type genomic DNA (Wt) were used as templates for controlling PCR reactions. **B** and **C**, Green-safe stained agarose gels showing PCR products obtained from the amplification using specific oligonucleotides (5' F and 3' R) of genes *slr1908*, *slr0042*, *sll1550*, *sll1271*, *sll0772*. Isolated genomic DNA of mutants transformed with the respective vectors was used as template (M). Wt- DNA template from the wild-type strain. C^- - PCR reactions in which the genomic DNA was replaced by water. L- GeneRuler 1 kb DNA Ladder (ThermoFisher Scientific).

The PCR product size corresponding to the insertion of the kanamycin resistance cassette is of approximately 2400 bp, while the expected product size for the native genomic DNA is of approximately 1400 bp, independently of the studied gene. Analysis of *Synechocystis* colonies resulting from the transformation of the pDC1841K plasmid indicated an incomplete replacement of *slr1841* by the antibiotic resistance cassette (Fig. 6A), even after growing in solid BG11 medium supplemented with high kanamycin concentrations. In contrast, the other five candidate genes were successfully knocked out as indicated by full chromosome segregation (Fig. 6B and 6C), and the resulting mutant strains were named Δ*1908*, Δ*1271*, Δ*0772*, Δ*0042* and Δ*1550*, for genes *slr1908*, *sll1271*, *sll0772*, *slr0042*, *slr1550,* respectively (generally referred throughout the work as knockout mutants). The impossibility to knockout gene *slr1841* indicates that the

encoded protein is essential under standard culture conditions, which is in agreement with other works that report the difficulty to generate mutated versions of this gene (Kowata *et al.* 2017; Qiu *et al.* 2021). This result is likely related to the function and abundance of the encoded protein: from the six proteins selected in this work, two are known to be expressed in standard culture conditions (Slr1841 and Slr1908) (Kowata *et al.* 2017), and Slr1841 is the most abundant protein in the outer membrane (Fig. 4C). However, a CRISPRi (interference) mutant was reported for gene *slr1841*, in which there is significant reduction of gene expression (knockdown) (Kojima and Okumura 2020). Characterization of the mutant revealed that cells lose approximately 70% of its outer membrane after *slr1841* gene downregulation, demonstrating the pivotal function of Slr1841 in *Synechocystis* outer membrane stability.

3.1.2- Knockout mutants' growth rates in standard culture conditions

To understand if the knockout of the genes encoding proteins containing SLH-OprB-domains promote changes in culture growth, the different strains were cultivated in standard liquid BG11 medium and their growth rates determined and compared to the wild-type strain (Fig. 7).

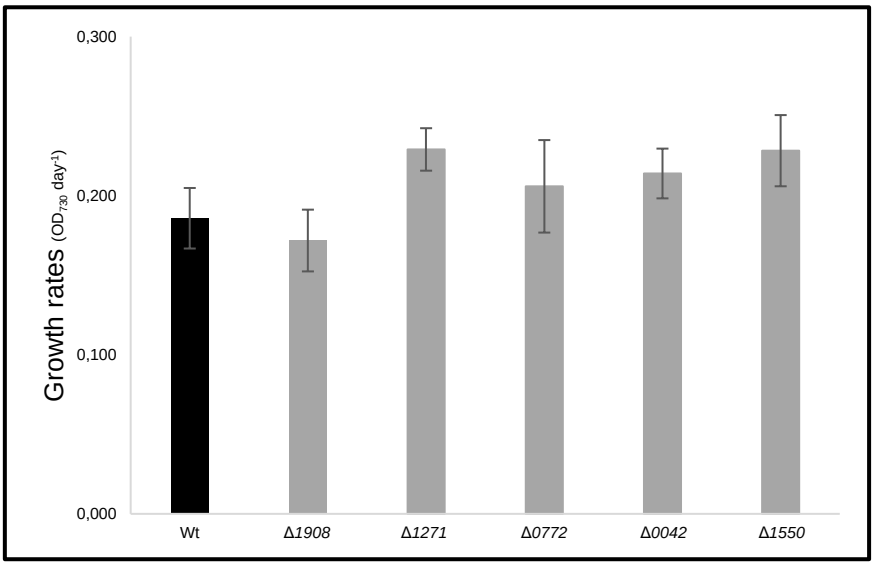


Figure 7. Knockout mutants' growth rates determined in cultures grown in liquid BG11 medium with a 16 h light/ 8 h dark cycle.

Cultures were grown in 96-well clear bottomed microplates at 30 ºC with a 16 h light (50 µmol photons m^{-2} s^{-1})/ 8 h dark cycle regime, with agitation, for 4 days. Every day, cell cultures were suspended and their optical density (OD_{730}) was measured on a microplate reader. Growth rates were determined between the first and fourth day of cultivation. Error bars represent the standard deviation of three independent biological replicates. No growth differences were found between the wild-type (Wt) and any mutant strain as determined by one way ANOVA ($p > 0.05$).

None of the investigated strains displayed significant differences in their growth rates. This result indicates that the mutated genes are not essential, and that their absence does not induce growth impairment, at least under the tested conditions.

3.1.3- Outer membrane and cell-free extracellular medium protein content

The proteins selected for investigation in this section of the work are highly abundant in the outer membrane. Therefore, the knockout of the respective encoding genes could result in outer membrane protein adaptations. Furthermore, the absence of major OMPs may also alter cell envelope integrity, which could result in unspecific leakage effects. To address these hypotheses, all the knockout mutants' outer membranes, and cell-free extracellular medium samples were isolated, separated by electrophoresis on SDS-polyacrylamide gels, and stained with PageBlue™ Staining Solution (Fig. 8).

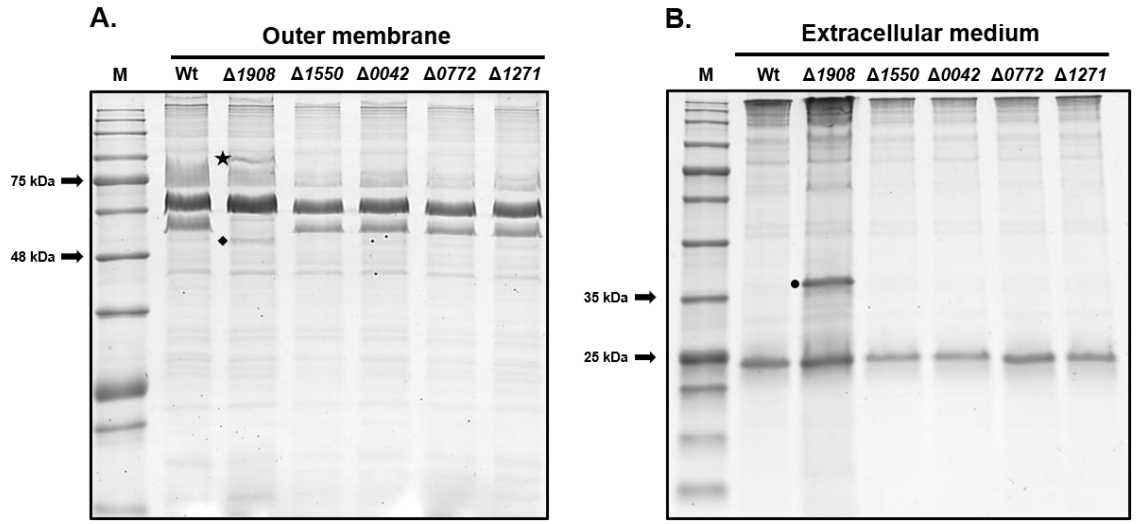


Figure 8. Analyses of the composition of the knockout mutants' outer membrane and cell-free extracellular medium.

A. PageBlue™ stained 12% (w/v) SDS-polyacrylamide gel showing the protein composition of isolated *Synechocystis* wild-type and mutant strains' outer membrane preparations. ★- FhuA (Sll1406); ◆- Sll1550. **B.** Protein profile of the concentrated cell-free extracellular medium from the wild-type and knockout mutants. Proteins were stained with PageBlue™ Staining Solution after separation in a 4-15% SDS-polyacrylamide gel. Sample loading is normalized to each culture cell density (OD_{730}), volume of cell-free medium concentrated and concentration factor. ●- FutA2 (Slr0513); M- NZYColour Protein Marker II (NZYTech); Wt- wild-type.

In agreement with the genetic modification introduced, the outer membrane protein preparation from the Δ*1908* mutant (Fig. 8A) lacks the protein band corresponding to the Slr1908 protein (cf. Fig. 4C). Nevertheless, two peptide bands of approximately 55 kDa and 95 kDa could be observed differentially accumulating in the mutant as compared to the wild-type. Mass spectrometry analysis identified them as

proteins Sll1550 and Sll1406, respectively. In line with the identification of Sll1550 in the outer membrane preparation of Δ*1908* mutant it is possible to observe that the corresponding band in mutant Δ*1550* is absent. Besides these differences, no further outer membrane protein alterations could be detected in the remaining mutant strains analysed here. This could result from low protein expression of proteins Slr0042, Sll0772 and Sll1271, and/or the fact that the respective protein bands separate together with other high abundant outer membrane proteins (it is worth highlighting that all proteins containing SLH-OprB-domains have approximately the same amino acid length (Fig. 4B)).

The protein composition in concentrated extracellular medium samples from the knockout mutants (Fig. 8B), was overall similar to that of the wild-type strain. Therefore, this result discards the possibility of a severe periplasmic protein content leakage phenotype. However, Δ*1908* shows the presence of an additional protein band with approximately 38 kDa, identified as Slr0513 by mass spectrometry. It was also observed that this mutant had an overall higher protein abundance when compared to the other strains.

It has been previously described that the knockout of the *slr1908* gene can induce the expression of other genes encoding proteins containing SLH-OprB-domains (Kowata *et al.* 2017; Agarwal *et al.* 2021). Further than altered gene expression, the present work demonstrates that Sll1550 protein accumulates in higher amounts in the Δ*1908* outer membrane. In addition, the two other proteins identified in the Δ*1908* mutant, Sll1406 and Slr0513, are known iron-import related proteins. Sll1406 is homologous to the FhuA protein from *E. coli* (Katoh *et al.* 2001). FhuA is one of the TonB-dependent transporters (TBDTs) localized in the outer membrane of Gram-negative bacteria (Katoh *et al.* 2001; Noinaj *et al.* 2010). TBDTs were found to mediate substrate uptake, mainly iron combined with siderophores (*e.g.* ferrichrome) or in inorganic free form, but also vitamins and carbohydrates (Noinaj *et al.* 2010). Qiu *et al*. demonstrated that the Sll1406 protein from *Synechocystis* is a TonB-dependent transporter together with three more proteins (Qiu *et al.* 2018). These TBDTs were suggested to have redundant functions, as single knockout mutants of each of them resulted in strains lacking any distinguishable phenotype (Qiu *et al.* 2018). However, a quadruple *Synechocystis* knockout mutant of all TBDTs showed a marked impairment in iron uptake, as the strain was almost completely unable to import iron siderophores, and showed a severe limitation in inorganic free iron uptake. Moreover, Slr0513 is annotated as the iron uptake protein A2 (FutA2), a component of the Fut iron uptake system. This is composed by two periplasmic binding proteins (FutA1 and FutA2), and two inner membrane proteins (FutB and FutC) (Katoh *et al.* 2001). The periplasmic proteins are iron binding proteins that

mediate iron transport (Katoh *et al.* 2001; Badarau *et al.* 2008). In *Synechocystis*, only the FutA2 protein was found in the periplasmic space, where it is the most abundant protein in the aqueous fraction, while the FutA1 protein was found to be absent from the periplasm and the inner membrane (Fulda *et al.* 2000; Tölle *et al.* 2002). The finding of increased abundance in iron uptake proteins in the Δ*1908* mutant is in agreement with the potential role proposed for the Slr1908 protein to work as a porin (Kowata *et al.* 2017). Kowata *et al.* showed that Slr1841, Slr1908 and the Slr0042 are responsible for up taking approximately 80% of inorganic ions (Kowata *et al.* 2017). Moreover, Slr1908 has also been suggested to work as an iron-selective porin (Qiu *et al.* 2021). Based on the results of this work and on literature reports, Δ*1908* was then selected for further studies to uncover its altered iron uptake phenotype, and to better understand the function of the Slr1908 protein in *Synechocystis*.

3.1.4- Characterization of the Δ*1908* mutant iron-related phenotype

To evaluate the role played by the Slr1908 protein in *Synechocystis* related to iron uptake, the growth of the wild-type and Δ*1908* strains was evaluated, using a microtiter-based assay. For that purpose, cells were cultivated either in a 16 h light/ 8 h dark cycle regimen, or in continuous light conditions. In the former case, cells were tested in two different setups: either pre-adapted in iron-limiting conditions for 7 days prior to cultivation, or without adaptation period. In all experimental setups, both strains were cultivated in liquid BG11 medium (control condition), and in BG11 medium with different iron composition: one lacking iron ammonium citrate (condition Ø), and the other with 2-fold excess iron ammonium citrate (condition 2x). During the experiment, OD_{730} was measured on a daily basis (Fig. 9).

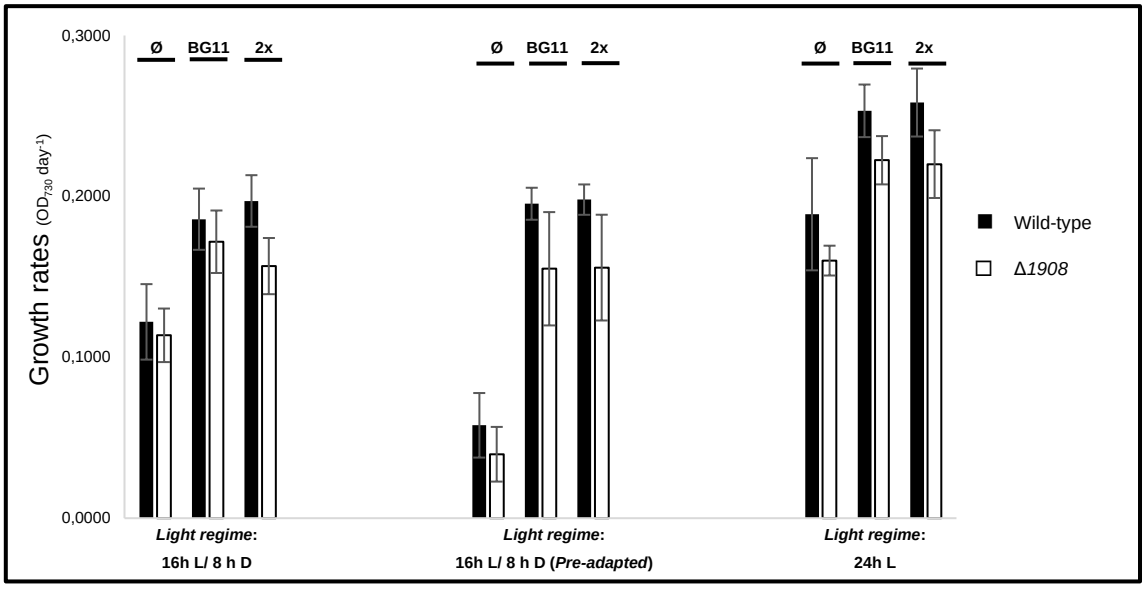


Figure 9. *Synechocystis* sp. PCC 6803 wild-type and Δ*1908* mutant growth rates in BG11 medium with modified iron ammonium citrate concentration, under different cultivation setups.

Cyanobacterial cells were cultivated in 96-well clear bottomed microplates at 30 ºC for 4 days. Standard BG11 medium was used as control condition (BG11), or in BG11 either lacking iron ammonium citrate (Ø) or in BG11 medium containing 2-fold excess iron ammonium citrate (2x). Different cultivation setups were tested: 1) cells were grown under a 16 h light (50 µmol photons m^{-2} s^{-1})/ 8 h dark cycle regime (16h L/ 8h D); 2) cells were previously pre-adapted for 7 days in BG11 medium without iron ammonium citrate, and then used as inoculum for the cultivation assay, under a 16 h light (50 µmol photons m^{-2} s^{-1})/ 8 h dark cycle regime (16h L/ 8h D (Pre-adapted)); 3) cells grown under constant light (24h L). Error bars represent the standard deviation of at least three independent biological replicates. No growth differences were found between the wild-type and the mutant strain when compared in the same combination of light cycle regime and iron availability as determined by one way ANOVA ($p > 0.05$).

As different enzymatic complexes involved in the light reactions of photosynthesis require iron as co-factor (e.g. photosystems I and II, cytochrome b_6f), different light regimes and iron-availability conditions were tested in this work. Overall, growth rates' analysis showed that cyanobacterial strains cultivated under continuous light grew faster than those in light/ dark cycles, as previously reported (De Rosa *et al.* 2015). Moreover, it was also possible to observe that cells cultivated in medium lacking iron ammonium citrate (Ø) had lower growth rates as to those cultivated in complete medium (BG11) or supplemented with extra amounts of iron ammonium citrate (2x), in agreement with previous reports (Qiu *et al.* 2021). Nevertheless, irrespectively of the condition analysed, strain Δ*1908* did not show significant differences in growth when compared to the wild-type. Altogether, these results indicate that under physiological conditions combining light regime and iron availability, the absence of Slr1908 does not induce significant growth impairment, which may suggest that Δ*1908* does not have an iron-content depleted phenotype. However, Slr1908 has been shown to selectively allow iron import (Qiu *et al.* 2021). In Qiu *et al.*, the strain used for characterization was generated by

constructing a knockdown mutant, in which *slr1908* gene expression was under the control of a copper-responsive promoter (Qiu *et al.* 2021). This strategy is different from what is reported here, in which part of the coding sequence of the *slr1908* gene was fully knocked out. Differences in mutant generation could therefore result in significantly different phenotypes. Still, this work further supports the role played by Slr1908 in iron uptake. Differential accumulation of proteins in the outer membrane (FhuA and Sll1550) and in the extracellular medium (FutA2) strongly indicate that iron uptake systems have been adapted to adjust for the absence of Slr1908. The higher abundance of FhuA in the outer membrane can result from an attempt to increase iron uptake by other routes, namely by the TonB-dependent transport system. In addition, FutA2 protein is known to bind inorganic iron, and its high accumulation in the extracellular medium may represent a strategy for iron scavenging from the medium, which would require further FutA2 internalization. Moreover, Sll1550 may also represent an additional mechanism for iron uptake: in fact, different reports show that *sll1550* gene expression is upregulated when *Synechocystis* wild-type cells are exposed to iron-limiting conditions (Hernandez-Prieto and Futschik 2012; Kopf *et al.* 2014).

3.1.5- LPS abundance in the cell-free extracellular medium

As the main objective of this part of the work was to study the amount of vesicles produced in mutants lacking proteins containing SLH-OprB-domains, the work was then focused on the characterization of the respective knockout mutants' phenotype regarding the release of EVs. LPS are structural components of the outer membrane, present in its outer leaflet. Therefore, the presence of this type of molecules in cell-free extracellular medium samples is considered a molecular marker for the detection of secreted EVs (Oliveira *et al.* 2016; Gonçalves *et al.* 2018). Thus, the various cyanobacterial strains were cultivated and the cell-free extracellular medium samples separated by electrophoresis and stained for their LPS content (Fig. 10).

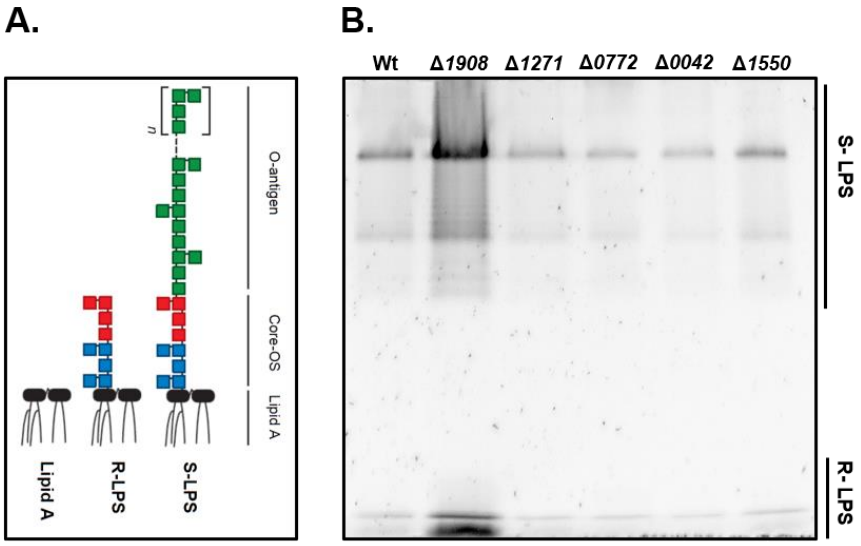


Figure 10. Analysis of the lipopolysaccharides (LPS) content in *Synechocystis* sp. PCC 6803 wild-type and knockout mutant strains in cell-free extracellular medium samples.

A. Schematic representation of the LPS structure in Gram-negative bacteria. S-LPS- smooth lipopolysaccharides; R-LPS- rough lipopolysaccharides. Figure adapted from (Whitfield and Trent 2014). **B.** Cyanobacterial strains were cultivated under standard conditions, and the growth medium was collected and concentrated after cultivation. Cell-free, concentrated samples were separated on 16% (w/v) SDS-polyacrylamide gels and stained with Pro-Q™ Emerald 300 Lipopolysaccharide Gel Stain Kit. Sample loading is normalized to each culture cell density (OD_{730}), volume of cell-free medium concentrated and concentration factor. Wt- wild-type.

Analyses of concentrated extracellular medium samples indicated that Δ*1908* is the only mutant strain showing more LPS abundance (both of the smooth- and rough-LPS forms) in the extracellular medium when compared to the wild-type strain (Fig. 10B). The increase of LPS in the extracellular medium is an indication of a possible higher release of EVs. For this reason, the Δ*1908* mutant strain was selected for further studies.

3.1.6- Δ*1908*: a strain with increased vesiculation phenotype

In order to characterize the EVs produced by Δ*1908* and to compare them with those released by the wild-type, EVs were isolated by a combination of ultrafiltration and ultracentrifugation. For characterization purposes, three methodologies were performed: 1) staining and quantification of LPS from the isolated EVs; 2) quantification of EVs by nanoparticle tracking analysis; and 3) morphology evaluation and size estimation by negatively stained, transmission electron microscopy analysis (Figs. 11 and 12).

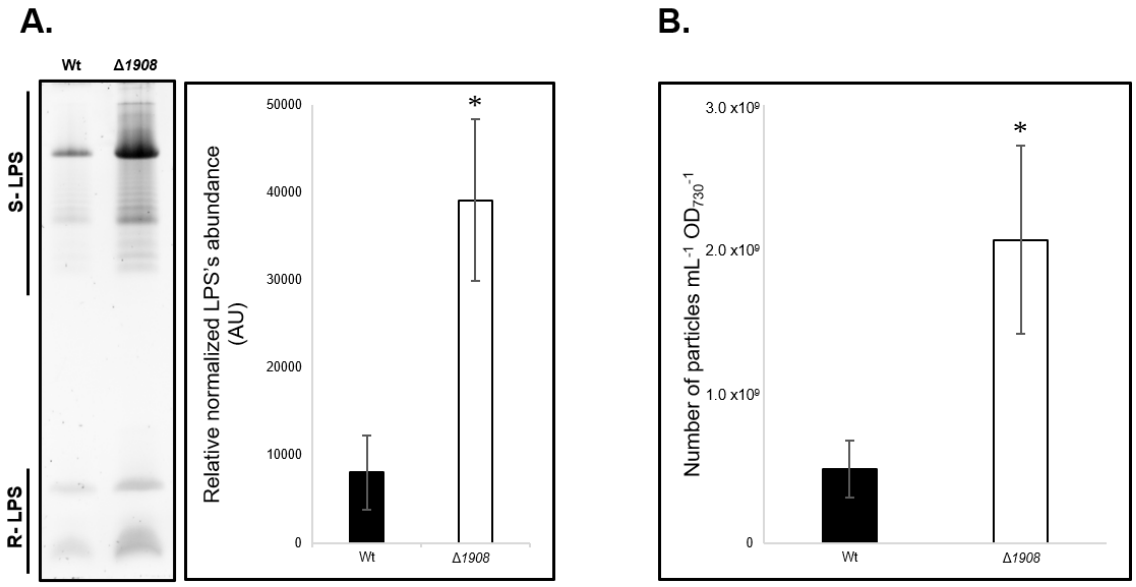


Figure 11. Analysis of the vesiculation capacity of *Synechocystis* sp. PCC 6803 wild-type and Δ*1908* strains. Cyanobacterial strains were cultivated under standard conditions and their EVs isolated by ultrafiltration and ultracentrifugation. **A.** EVs samples from wild-type (Wt) and Δ*1908* mutant were separated by electrophoresis on 16% (w/v) SDS-polyacrylamide gel and stained with Pro-Q™ Emerald 300 Lipopolysaccharide Gel Stain. Sample loading is normalized to each culture cell density (OD_{730}), volume of cell-free medium concentrated and concentration factor. LPS band intensity was quantified by densitometry using the ImageJ software, resulting in the graph shown onto the right-hand side. S-LPS- smooth lipopolysaccharides; R-LPS- rough lipopolysaccharides; AU- arbitrary units. **B.** Particle concentration determination of the isolated EVs samples by nanoparticle tracking analysis. Error bars represent the standard deviation of three independent biological replicates. *, $p < 0.05$ as determined by one way ANOVA.

In agreement with the analysis of complete extracellular medium concentrated samples (Fig. 10B), analysis of the LPS content in EVs samples, followed by densitometry quantification, indicated that Δ*1908* contains approximately 5-fold more LPS then the wild-type strain samples (Fig. 11A). Furthermore, nanoparticle tracking analysis allowed for the quantification of the total amount of nano-sized particles in the samples (Fig. 11B). This technique shows that Δ*1908* mutant strain releases up to 4-fold more nanoparticles than the parental strain. These results strongly suggest that Δ*1908* is a hypervesiculating strain.

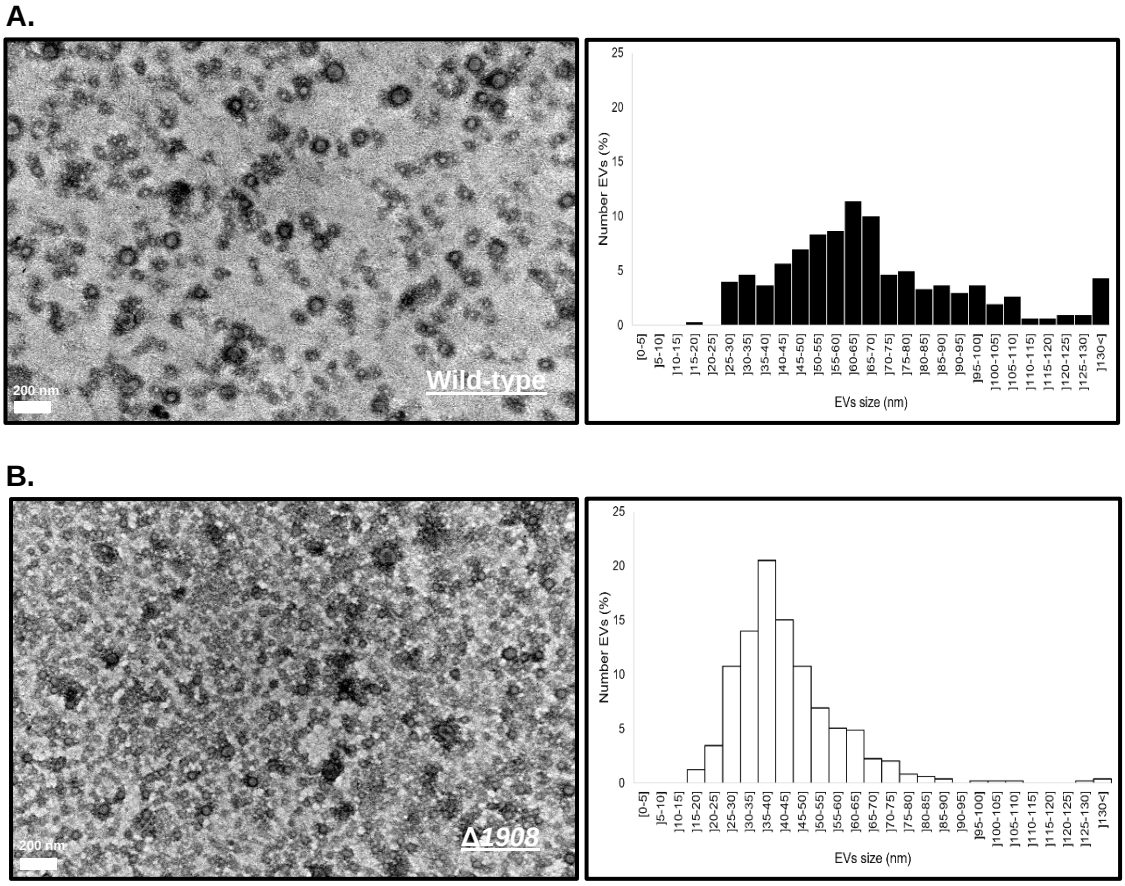


Figure 12. Morphology and size distribution analysis of extracellular vesicles isolated from the *Synechocystis* sp. PCC 6803 wild-type and Δ*1908* mutant based on transmission electron microscopy.

Cyanobacterial strains were cultivated under standard conditions and their EVs isolated by ultrafiltration and ultracentrifugation. EVs from the *Synechocystis* wild-type (**A**.) and Δ*1908* mutant (**B.**) were negatively stained using 1% (w/v) uranyl acetate and visualized by transmission electron microscopy (TEM). EVs size from both cultures were measured using the ImageJ software, resulting in the histograms shown onto the right-hand side. Size bar of 200 nm in each micrograph. Histograms showing particle size distribution of EVs samples from the two cyanobacterial strains are presented. EVs were separated in 5 nm size groups, distributed between 0 and 130 nm, and in a group comprising those with a size higher than 130 nm. Vesicle diameter was determined by direct measurement from electron micrographs of three independent biological replicates. Abundance of each size group is presented as relative figures, i.e. number of vesicles with a given diameter range relative to the total number of vesicles measured.

Negatively stained transmission electron micrographs of isolated EVs (Fig. 12) show the accumulation of nano-sized spherical structures that resemble those of EVs reported earlier for *Synechocystis* (Pardo *et al.* 2015; Oliveira *et al.* 2016) and other Gram-negative bacteria (Lima *et al.* 2020). In line with LPS and nanoparticle tracking analyses, electron micrographs further support the higher vesiculation capacity of Δ*1908*. In addition, this technique also allowed to detect shifts in size of the released EVs. Wild-type EVs have a broad diameter distribution, and more than 50% of the measured vesicles range between 45 and 75 nm in diameter. In contrast, EVs produced by Δ*1908* have a more homogeneous size distribution, with approximately 50% of the

measured EVs with a diameter between 30 and 45 nm (Fig. 12). However, the biological aspects accounting for the differences in EVs' size between the wild-type and the mutant strain remain unknown. Still, another line of evidence supporting the superior vesiculation phenotype of Δ*1908* is the global higher protein abundance in concentrated extracellular medium samples when compared to those of the wild-type (Fig. 8B), as EVs are known to mimic the cell envelope structure and to transport proteins in their lumen (Lima *et al.* 2020).

The increase in vesicles' release by Δ*1908* is in line with the proposed biogenesis mechanism for Gram-negative bacteria, based on the modulation of links between the outer membrane and the remaining cell envelope components. This suggests that cyanobacteria can release EVs following this particular EVs production route. Nevertheless, Δ*1908* also shows extensive adaptations to iron uptake. Therefore, it should not be discarded that mutant cells may be using EVs as an alternative iron uptake system. In this regard, it has been suggested that EVs can be loaded with proteins or other molecules to scavenge iron from the extracellular medium, and later be internalized by the cells (Kulp and Kuehn 2010; Prados-Rosales *et al.* 2014; Schwechheimer and Kuehn 2015; Lin *et al.* 2017). Once the protein content from the isolated EVs was not analysed in this work, further testing is needed to clarify the roles played by the EVs in the Δ*1908*.

3.2- Modulation of periplasmic pressure resulting from the accumulation of heterologous proteins

3.2.1- *Synechocystis* mutant strains expressing sfGFP

According to proposed EVs biogenesis models, an overall increase in the amount of molecules in the periplasmic space will lead to a build-up turgor pressure that, ultimately, pushes the outer membrane to the extracellular medium, resulting in an increased release of EVs (Kulp and Kuehn 2010; Schwechheimer and Kuehn 2015; Lima *et al.* 2020). In order to study this hypothesis in the cyanobacterium *Synechocystis*, it was decided to express and target the heterologous, reporter protein superfolder-green fluorescent protein (sfGFP) to the periplasmic space. To control sfGFP translocation to the periplasm, the signal peptide of the native FutA2 protein was selected (Polyviou *et al.* 2018). Moreover, to modulate the amount of sfGFP expressed in cells, two constitutive promoters driving transcription with different strengths were used. Thus, the relatively weak promoter of the native *rbcL* gene (P_{rbcL}) (Huang *et al.* 2010), and the strong and synthetic promoter $P_{trc.x.lacO}$ (Ferreira *et al.* 2018) were chosen. Assembly of the different parts (promoter; signal peptide; sfGFP encoding gene) was performed by

overlap extension PCR, and the resulting constructs transformed into *Synechocystis*, targeting the neutral site 15 (Pinto *et al.* 2015) by double homologous recombination (Fig. 13A). This work was carried out by other members in the group, who also confirmed expression of sfGFP by confocal microscopy analysis (Fig. 13B) (Lima, Matinha-Cardoso, *et al.*, unpublished work). Thus, 4 fully segregated, sfGFP-expressing *Synechocystis* strains were studied, namely: L::noSP (Promoter: $P_{trc.x.lacO}$; FutA2 signal peptide: absent); L::Fut (Promoter: $P_{trc.x.lacO}$; FutA2 signal peptide: present), R::noSP (Promoter: P_{rbcL}; FutA2 signal peptide: absent), and R::Fut (Promoter: P_{rbcL}; FutA2 signal peptide: present) (see more details in Table 1).

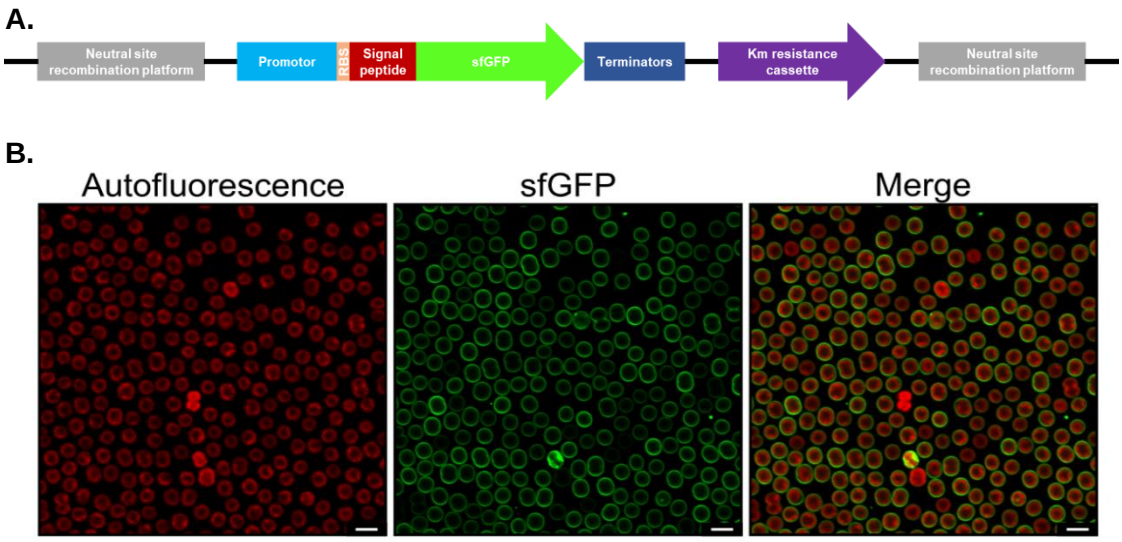


Figure 13. Design of the constructs used to generate *Synechocystis* sp. PCC 6803 mutant strains expressing sfGFP and microscopic analysis of the respective fluorescent signal from strain L::Fut.

A. Schematic representation of the sfGFP-based constructs used in this work. Gray boxes- specific recombination platforms for the *Synechocystis* genomic neutral site 15; Light blue- promotor box, either $P_{trc.X.lacO}$ or P_{rbcL}; Light brown- ribosome binding site (RBS); Red- Signal peptide box, which was either present (sfGFP translocated to the periplasm) or absent (sfGFP remains in the cytoplasm); Green- open reading frame encoding the superfolder-green fluorescent protein (sfGFP); Dark blue- terminators sequence; Purple- kanamycin resistance cassette. **B.** Confocal micrographs of L::Fut strain ($P_{trc.x.lacO}$; with signal peptide) showing the cells' autofluorescence signal obtained from the cyanobacterial photosynthetic pigments (Exc. 633 nm; Em. 640-680 nm) and the sfGFP derived fluorescence signal (Exc. 488 nm; Em. 495-560 nm). Scale bar: 5 µm. Micrographs kindly provided by Paulo Oliveira.

To understand if expression of the protein of interest could cause differences in growth in the *Synechocystis* mutants, wild-type and mutant strains were tested in a microtiter-based assay under standard culture conditions (Fig. 14).

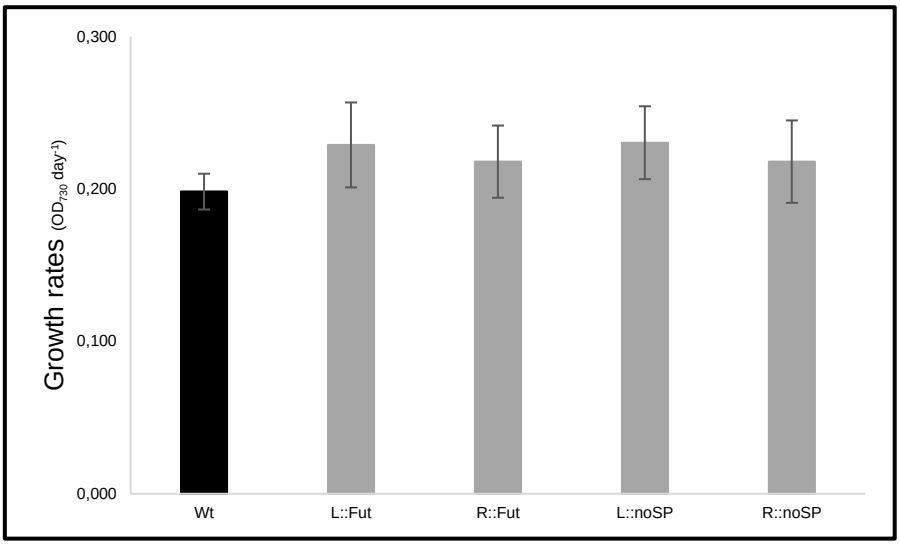


Figure 14. *Synechocystis* sp. PCC 6803 wild-type and sfGFP-expressing mutant strains growth rates determined from cultures grown under standard conditions.

Cultures were grown in 96-well clear bottomed microplates at 30 ºC with a 16 h light (50 µmol photons m^{-2} s^{-1})/ 8 h dark cycle regime, with agitation, for 4 days. Every day, cell cultures were suspended and their optical density (OD_{730}) was measured on a microplate reader. Growth rates were determined between the first and fourth day of cultivation. Error bars represent the standard deviation of three independent biological replicates. No growth differences were found between the wild-type and any mutant strain as determined by one way ANOVA ($p > 0.05$). Wt- wild-type. L::Fut- Promoter: $P_{trc.x.lacO}$; FutA2 Signal peptide: present. R::Fut- Promoter: P_{rbcL}; FutA2 Signal peptide: present. L::noSP- Promoter: $P_{trc.x.lacO}$; FutA2 Signal peptide: absent. R::noSP- Promoter: P_{rbcL}; FutA2 Signal peptide: absent.

Analysis of the mutant strains' growth rates indicated that none of them shows significantly different growth when compared to the wild-type strain (Fig. 14). This result suggests that the introduced constructions, and the resulting expressed protein, do not impact cyanobacterial growth.

3.2.2- Analysis of intra- and extracellular fluorescence intensity signal

Once the mutant strains were shown not to be affected by the respective inserted constructions, the sfGFP fluorescence levels of the various strains were then measured on cells cultivated in standard conditions for 4 days on microtiter plates. To assess the amount of sfGFP present in cells and in the growth medium, the intra- and extracellular fluorescence signals were analysed (Fig. 15).

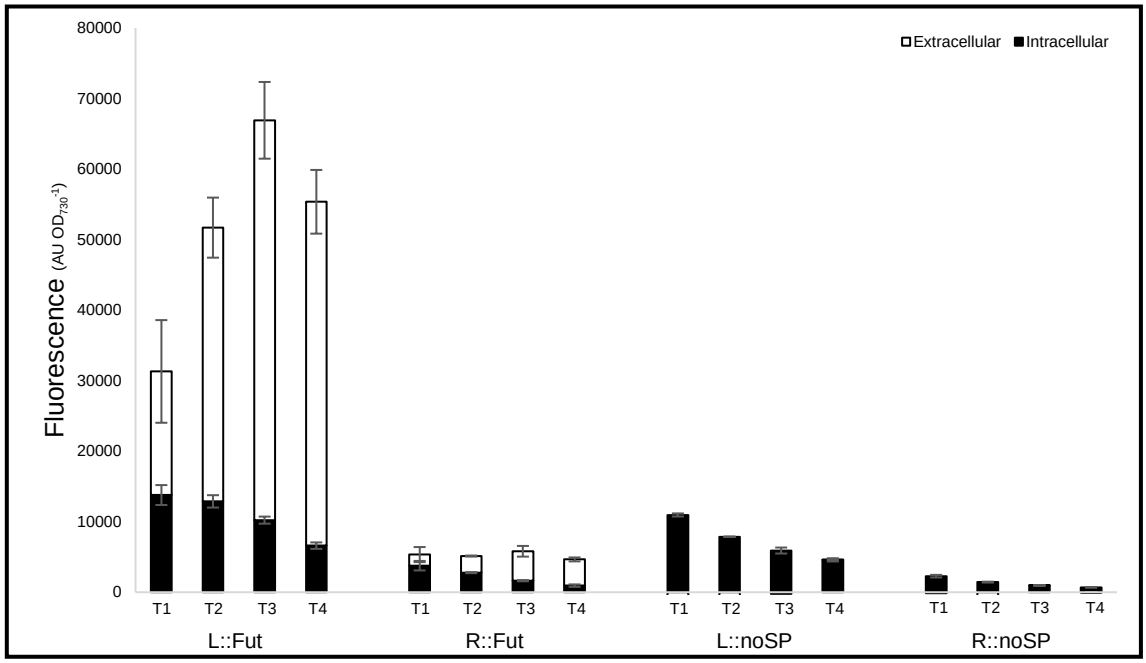


Figure 15. Intra- and extracellular sfGFP fluorescence signal determined for the *Synechocystis* sp. PCC 6803 strains L::Fut ($P_{trc.x.lacO}$; with FutA2 signal peptide), R::Fut (P_{rbcL}; with FutA2 signal peptide), L::noSP ($P_{trc.x.lacO}$; without FutA2 signal peptide), and R::noSP (P_{rbcL}; without FutA2 signal peptide).

Cells were grown in four 96-well clear bottomed microplates at 30 ºC with a 16 h light (50 µmol photons $m^{-2} s^{-1}$)/ 8 h dark cycle regime for 4 days (T1 to T4). Every day, cells in one of the microplates were analysed for their OD_{730}, and total and intracellular fluorescence. Wild-type cells were also included in the analysis, and the intrinsic autofluorescence signal was subtracted from the fluorescence measurements, which were then normalized by cell density measured as OD_{730}. Extracellular fluorescence was calculated by subtracting the intracellular fluorescence to the total fluorescence measured. AU- arbitrary units. Error bars represent the standard deviation of three independent biological replicates.

This experiment allowed to detect sfGFP fluorescence signal in all mutant strains, further supporting that the assembled constructs are functional in *Synechocystis*. Nevertheless, sfGFP signal could only be detected in the extracellular space of strains L::Fut and R::Fut. This result is in agreement with the fact that sfGFP in both strains is fused with the FutA2 signal peptide, which determines protein translocation to the periplasm (Fig. 13B), and eventually to the growth medium (cf. Fig. 8B), suggesting that the signal peptide is essential for protein secretion. Absence of signal peptide determines therefore that the protein remains in the cytoplasm. Moreover, it was also possible to observe that strains harbouring constructs including the $P_{trc.x.lacO}$ promoter show significantly higher fluorescence signal than the respective strains in which sfGFP expression is under the control of P_{rbcL}. This is also in agreement with the described relative transcription strength of these two promoters determined by Huang *et al.* who report a difference of approximately 4-fold (Huang *et al.* 2010). Another important observation is that the total amount of fluorescence signal was found to be higher in *Synechocystis* strains expressing sfGFP fused to the FutA2 signal peptide (L::Fut and

R::Fut) than those in which sfGFP did not contain signal peptide (L::noSP and R::noSP). These results were somewhat unexpected, and several factors could account for the observed differences. On one hand, constructs in which the sf*gfp* gene are fused with the coding sequence of the FutA2 signal peptide could alter mRNA synthesis and/or stability as compared to the condition without signal peptide (Tietze and Lale 2021). On the other hand, presence of the FutA2 coding sequence on the mRNA may also have an impact on the rate of protein synthesis (Formighieri and Melis 2016). In addition, heterologous protein stability may also represent a factor underlying the observed differences (Zhang *et al.* 2021). Nevertheless, sfGFP accumulation in the cytoplasm can also trigger a feedback control mechanism that reduces protein expression, which is overcome in the mutants as sfGFP is secreted to the extracellular medium. Further work needs to be carried out to clarify these results (*e.g.* analysis of sf*gfp* transcript levels in the different *Synechocystis* mutant strains, and even evaluation of sfGFP protein half-life by pulse-chase analysis).

3.2.3- Analysis of EVs released by the sfGFP-expressing *Synechocystis* strains

As the main goal of this section of the work was to study the amount and cargo composition of EVs released by strains with modulated periplasmic pressure, it was decided to focus on the extracellular medium of these strains. In Fig. 15, it is possible to observe that the amount of sfGFP fluorescence signal in the extracellular medium increases during cultivation. Therefore, 600 mL cultures were grown under standard conditions for 4 days, and the extracellular medium collected. This was then filtered to remove any contaminating cells, and a part was concentrated without any further processing (includes both soluble biomolecules and EVs released by cyanobacterial cells), while the remaining part was used for EVs isolation. Western blot analysis of the sfGFP protein levels was then carried out in these samples derived from the extracellular growth medium (Fig. 16).

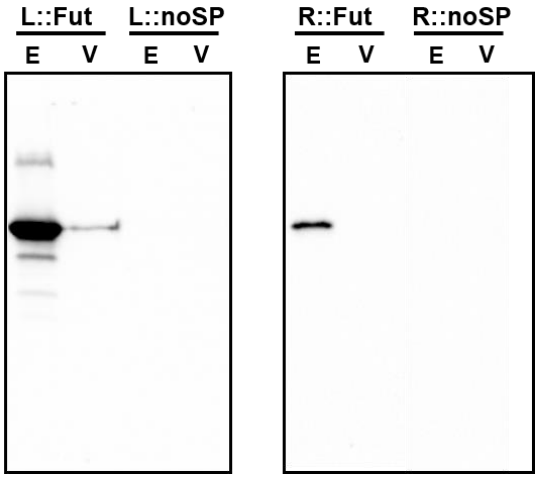


Figure 16. Western blot analysis of the sfGFP protein levels present in the extracellular medium and in isolated vesicles of the sfGFP-expressing *Synechocystis* sp. PCC 6803 mutant strains.

Cyanobacterial strains L::Fut ($P_{trc.x.lacO}$; with FutA2 signal peptide), R::Fut (P_{rbcL}; with FutA2 signal peptide), L::noSP ($P_{trc.x.lacO}$; without FutA2 signal peptide), and R::noSP (P_{rbcL}; without FutA2 signal peptide) were cultivated under standard conditions for 4 days, and the respective extracellular medium (E) concentrated. Extracellular vesicles (V) were also isolated. Samples were loaded onto 16% (w/v) SDS-polyacrylamide gels, and separated by electrophoresis. Prior to loading, samples were normalized to each culture cell density (OD_{730}), volume of cell-free medium concentrated and concentration factor.

L::Fut and R::Fut, but not L::noSP or R::noSP, accumulate sfGFP in the extracellular medium, which is in agreement with fluorescence measurements (Fig. 15). Interestingly, sfGFP protein was also detected in isolated EVs from strain L::Fut. This result shows that the cyanobacterial EVs' protein cargo composition can be customized with heterologous proteins, simply by translocating the protein of interest to the bacterial periplasm as previously shown for other Gram-negative bacteria (Kesty and Kuehn 2004). In contrast, sfGFP protein could not be detected in vesicular fractions of R::Fut, L::noSP or R::noSP (even when exposing the blots for long periods – data not shown). These observations suggest that only very high levels of protein in the periplasmic space (Fig. 15) can lead to encapsulation of the target protein into EVs.

Quantification by densitometry analysis of the sfGFP-protein signal from the Western blot carried out in three independent biological replicates showed that only about 10% of heterologous protein is released to the extracellular medium in the form of EVs. The molecular mechanism responsible for the EVs-independent sfGFP secretion to the extracellular medium is not known. Nevertheless, there are indications in the literature that periplasmic proteins in the cyanobacterium *Synechococccus elongatus* are secreted via the type IV-pilus secretion system, which is mainly responsible for the assembly of motility appendages in cyanobacteria (Yegorov *et al.* 2021). Besides this possibility, one cannot exclude the existence of other protein channels that may facilitate

protein translocation from the periplasm to the extracellular space, since the knowledge of the outer membrane protein composition and respective transport mechanisms are still poorly described in cyanobacteria.

Next, the amount of EVs produced by each strain was determined. To that end, isolated EVs samples were loaded on SDS-polyacrylamide gels and separated by electrophoresis, followed by the detection of their LPS content (Fig. 17).

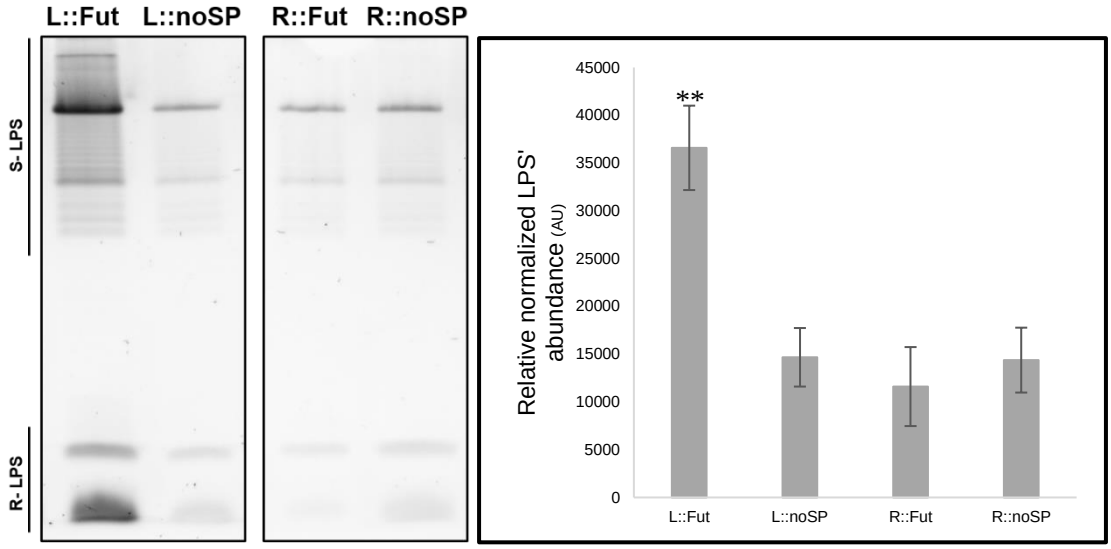


Figure 17. Analysis of the vesiculation capacity of the sfGFP-expressing *Synechocystis* sp. PCC 6803 mutants. Cyanobacterial strains were cultivated under standard conditions and their EVs isolated by ultrafiltration and ultracentrifugation. EVs samples were separated by electrophoresis on 16% (w/v) SDS-polyacrylamide gel and their LPS stained with Pro-Q™ Emerald 300 Lipopolysaccharide Gel Stain. Sample loading is normalized to each culture cell density (OD_{730}), volume of cell-free medium concentrated and concentration factor. Despite being displayed separately, EVs samples shown in the photographs were loaded on the same gel. LPS band intensity was quantified by densitometry using the ImageJ software (graph on the right-hand side). S-LPS- smooth lipopolysaccharides; R-LPS- rough lipopolysaccharides; AU- arbitrary units. Error bars represent the standard deviation of three independent biological replicates. **, $p < 0.01$ when comparing the L::Fut to any of the other mutant strains, determined by one way ANOVA.

From the four strains, L::Fut showed the highest LPS abundance. While L::noSP, R::Fut and R::noSP presented approximately the same quantity of LPS, L::Fut samples contain approximately 2.5-fold more LPS than any of the other 3 mutant strains (Fig. 17). This result strongly suggests that L::Fut significantly produces more EVs than the other tested mutants.

Based on the work shown here, it was possible to confirm that in cyanobacteria heterologous protein secretion to the extracellular space is dependent on the existence of a signal peptide that ensures protein translocation to the periplasm (Russo *et al.* 2019). In addition, the level of heterologous protein expression is also a key aspect for determining the amount of protein reaching the extracellular medium. In this regard, the amount of protein accumulating in the periplasm seems to trigger EVs formation and

release. These results are in agreement with the model involving high periplasmic pressure at the basis of EVs biogenesis (Kulp and Kuehn 2010; Schwechheimer and Kuehn 2015; Lima *et al.* 2020).

4- Conclusion and Future Perspectives

The current work focused on the identification of players and mechanisms involved in the biogenesis of EVs in cyanobacteria, having as point of departure two previously proposed EVs biogenesis mechanisms in Gram-negative bacteria. To achieve this goal two independent approaches were followed, and the main take-home messages from each section are listed below.

1) *Modulation of links between the outer membrane and the remaining cell envelope components*

- **I.** Slr1841 is an essential protein, as demonstrated by the impossibility to generate the corresponding knockout mutant;
- **II.** Mutants lacking the genes encoding the proteins Slr0042, Sll1550, Sll1271 and Sll0772 lack any observable phenotype while grown in standard conditions;
- **III.** Δ*1908* mutant strain shows an iron-uptake adapted phenotype due to the higher accumulation of the iron uptake proteins FhuA and FutA2. However, no growth impairment was observed in different combinations of light regime and iron availability;
- **IV.** Δ*1908* mutant displays a hypervesiculating phenotype, and the resulting EVs are smaller than those released by the wild-type strain.

2) *Modulation of periplasmic pressure resulting from the accumulation of heterologous proteins*

- **I.** Presence of a signal peptide is a key requisite for protein translocation to the periplasm, and further to the extracellular medium;
- **II.** It is possible to load heterologous proteins into *Synechocystis* EVs;
- **III.** High accumulation of protein in the periplasm can increase vesiculation capacity in *Synechocystis*.

Altogether, these results **confirm that the biogenesis mechanisms for EVs production in *Synechocystis*, and most likely other cyanobacterial strains, follow the same basic principles proposed for other Gram-negative bacteria**.

The work presented here contributes to expand the knowledge regarding EVs production in cyanobacteria. It shows for the first time that it is possible of tailoring cyanobacterial EVs content with proteins of interest, simply by translocating it to the periplasmic space. Although possible, further optimization is needed, as indicated by the high leakage of the reporter sfGFP through the outer membrane into the extracellular medium, and by the required high levels of protein expression. Thus, identification of the respective secretion system and its subsequently downregulation will possibly allow to

engineer a strain capable of higher EV loading capacity, demanding less protein overexpression. Moreover, it is also possible to envisage a more refined EVs loading strategy, making use of split protein technology, which would allow more efficient protein loading into EVs, and concomitantly reduce protein expression. Such a system has already been described for *E. coli* EVs: using the SpyCatcher/SpyTag bioconjugation system it was possible to generate a synthetic linkage between the protein of interest and an abundant EV protein (outer membrane proteins), leading to efficient loading of EVs (Alves *et al.* 2016). However, EVs-protein cargo tailoring and EVs production capacity are two aspects that must be carefully considered in combination when engineering cyanobacteria for optimized EVs as biotechnological tools, for example, as a nanocarrier of target proteins to defined hosts, or as protecting capsules of target molecules. In this regard, the constructs described in this work ($P_{trc.X.lacO}$::*futA2* SP::sfGFP and P_{rbcL}::*futA2* SP::sfGFP) have already been inserted into the background of the Δ*1908* mutant strain. The goals of this test are to understand if it is viable to generate a *Synechocystis* strain with even higher vesiculation capacity, and if it will be possible to promote loading of sfGFP, expressed in moderate levels, in EVs of a hypervesiculating strain. Nevertheless, Δ*1908* mutant strain showed extensive iron uptake adaptations, and so, further studies are needed to understand if the EVs can play a role in iron scavenging in *Synechocystis* (e.g. wild-type growth evaluation in iron depleted media supplemented with EVs from the Δ*1908* strain and wild-type previously grown in iron depleted conditions). This also highlights that fundamental questions regarding the biology of EVs in cyanobacteria remain to be addressed. In conclusion, cyanobacteria may definitely become attractive models for the sustainable production of EVs with tailored protein cargo, but that will require deep characterization of their composition, biological roles, and biogenesis mechanisms.

5- References

Abed, R. M. M., Dobretsov, S., and Sudesh, K. **2009**. Applications of cyanobacteria in biotechnology, *J. Appl. Microbiol.*, 106: 1-12.

Agarwal, R., Choudhury, S. D., and Narayana Rao, A. V. S. S. **2021**. Iron acquisition across outer membrane: The role of major outer membrane protein Slr1908 under iron supplemented conditions in *Synechocystis* 6803, *bioRxiv*: 2021.01.14.426630.

Alves, N. J., Turner, K. B., Medintz, I. L., and Walper, S. A. **2016**. Protecting enzymatic function through directed packaging into bacterial outer membrane vesicles, *Scientific Reports*, 6: 24866.

Badarau, A., Firbank, S. J., Waldron, K. J., Yanagisawa, S., Robinson, N. J., Banfield, M. J., and Dennison, C. **2008**. FutA2 Is a ferric binding protein from *Synechocystis* PCC 6803, *J. Biol. Chem.*, 283: 12520-27.

Bauwens, A., Kunsmann, L., Karch, H., Mellmann, A., and Bielaszewska, M. **2017**. Antibiotic-mediated modulations of outer membrane vesicles in enterohemorrhagic *Escherichia coli* O104:H4 and O157:H7, *Antimicrob.l Agents Chemother.*, 61: e00937-17.

Berman-Frank, I., Lundgren, P., and Falkowski, P. **2003**. Nitrogen fixation and photosynthetic oxygen evolution in cyanobacteria, *Res. Microbiol.*, 154: 157-64.

Bernadac, A., Gavioli, M., Lazzaroni, J.-C., Raina, S., and Lloubès, R. **1998**. *Escherichia coli tol-pal* mutants form outer membrane vesicles, *J. Bacteriol.*, 180: 4872-78.

Biller, S. J., Schubotz, F., Roggensack, S. E., Thompson, A. W., Summons, R. E., and Chisholm, S. W. **2014**. Bacterial vesicles in marine ecosystems, *Science*, 343: 183-86.

Cantine, M. D., and Fournier, G. P. **2018**. Environmental adaptation from the origin of life to the last universal common ancestor, *Orig. Life Evol. Biosph.*, 48: 35-54.

Cascales, E., Bernadac, A., Gavioli, M., Lazzaroni, J.-C., and Lloubes, R. **2002**. Pal lipoprotein of *Escherichia coli* plays a major role in outer membrane integrity, *J. Bacteriol.*, 184: 754-59.

Cavalier-Smith, T. **2006**. Cell evolution and Earth history: stasis and revolution, *Philos. Trans. R. Soc. B: Biol. Sci.*, 361: 969-1006.

Chatterjee, K. R., Gupta, N. N. D., and De, M. L. **1959**. Electron microscopic observations on the morphology of *Mycobacterium leprae*, *Exp. Cell Res.*, 18: 521-27.

Choi, H.-i., Kim, M., Jeon, J., Han, J. K., and Kim, K.-s. **2017**. Overexpression of MicA induces production of OmpC-enriched outer membrane vesicles that protect against *Salmonella challenge*, *Biochem. Biophys. Res. Commun.*, 490: 991-96.

Coelho, C., and Casadevall, A. **2019**. Answers to naysayers regarding microbial extracellular vesicles, *Biochem. Soc. Trans.*, 47: 1005-12.

Confer, A. W., and Ayalew, S. **2013**. The OmpA family of proteins: Roles in bacterial pathogenesis and immunity, *Vet. Microbiol.*, 163: 207-22.

Cui, Y., Gao, J., He, Y., and Jiang, L. **2020**. Plant extracellular vesicles, *Protoplasma*, 257: 3-12.

De Rosa, E., Checchetto, V., Franchin, C., Bergantino, E., Berto, P., Szabò, I., Giacometti, G. M., Arrigoni, G., and Costantini, P. **2015**. [NiFe]-hydrogenase is essential for cyanobacterium *Synechocystis* sp. PCC 6803 aerobic growth in the dark, *Scientific Reports*, 5: 12424.

De, S. N. **1959**. Enterotoxicity of bacteria-free culture-filtrate of *Vibrio cholerae*, *Nature*, 183: 1533-34.

Deatherage, B. L., Lara, J. C., Bergsbaken, T., Barrett, S. L. R., Lara, S., and Cookson, B. T. **2009**. Biogenesis of bacterial membrane vesicles, *Mol. Microbiol.*, 72: 1395-407.

Denise, R., Abby, S. S., and Rocha, E. P. C. **2020**. The evolution of protein secretion systems by co-option and tinkering of cellular machineries, *Trends Microbiol.*, 28: 372-86.

Fais, S., O'Driscoll, L., Borras, F. E., Buzas, E., Camussi, G., Cappello, F., Carvalho, J., Cordeiro da Silva, A., Del Portillo, H., El Andaloussi, S., Ficko Trček, T., Furlan, R., Hendrix, A., Gursel, I., Kralj-Iglic, V., Kaeffer, B., Kosanovic, M., Lekka, M. E., Lipps, G., Logozzi, M., Marcilla, A., Sammar, M., Llorente, A., Nazarenko, I., Oliveira, C., Pocsfalvi, G., Rajendran, L., Raposo, G., Rohde, E., Siljander, P., van Niel, G., Vasconcelos, M. H., Yáñez-Mó, M., Yliperttula, M. L., Zarovni, N., Zavec, A. B., and Giebel, B. **2016**. Evidence-based clinical use of nanoscale extracellular vesicles in nanomedicine, *ACS Nano*, 10: 3886-99.

Ferreira, E. A., Pacheco, C. C., Pinto, F., Pereira, J., Lamosa, P., Oliveira, P., Kirov, B., Jaramillo, A., and Tamagnini, P. **2018**. Expanding the toolbox for *Synechocystis* sp. PCC 6803: validation of replicative vectors and characterization of a novel set of promoters, *Synth. Biol.*, 3: ysy014.

Florez, C., Raab, J. E., Cooke, A. C., and Schertzer, J. W. **2017**. Membrane distribution of the *Pseudomonas* quinolone signal modulates outer membrane vesicle production in *Pseudomonas aeruginosa, mBio*, 8: e01034-17.

Formighieri, C., and Melis, A. **2016**. Sustainable heterologous production of terpene hydrocarbons in cyanobacteria, *Photosynth. Res.*, 130: 123-35.

Fujisawa, T., Narikawa, R., Maeda, S.-i., Watanabe, S., Kanesaki, Y., Kobayashi, K., Nomata, J., Hanaoka, M., Watanabe, M., Ehira, S., Suzuki, E., Awai, K., and Nakamura, Y. **2016**. CyanoBase: a large-scale update on its 20th anniversary, *Nucleic Acids Res.*, 45: D551-D54.

Fulda, S., Huang, F., Nilsson, F., Hagemann, M., and Norling, B. **2000**. Proteomics of *Synechocystis* sp. strain PCC 6803 identification of periplasmic proteins in cells grown at low and high salt concentrations, *Eur. J. Biochem.*, 267: 5900-07.

Goemans, C., Denoncin, K., and Collet, J.-F. **2014**. Folding mechanisms of periplasmic proteins, *Biochim. Biophys Acta - Mol. Cell Res.*, 1843: 1517-28.

Gonçalves, C. F., Lima, S., Tamagnini, P., and Oliveira, P. **2019**. 'Chapter 18 - Cyanobacterial secretion systems: Understanding fundamental mechanisms toward technological applications.' in A. K. Mishra, D. N. Tiwari and A. N. Rai (eds.), *Cyanobacteria* (Academic Press), 359-81.

Gonçalves, C. F., Pacheco, C. C., Tamagnini, P., and Oliveira, P. **2018**. Identification of inner membrane translocase components of TolC-mediated secretion in the cyanobacterium *Synechocystis* sp. PCC 6803, *Environ. Microbiol.*, 20: 2354-69.

Haurat, M. F., Aduse-Opoku, J., Rangarajan, M., Dorobantu, L., Gray, M. R., Curtis, M. A., and Feldman, M. F. **2011**. Selective sorting of cargo proteins into bacterial membrane vesicles, *J. Biol. Chem.*, 286: 1269-76.

Heidorn, T., Camsund, D., Huang, H.-H., Lindberg, P., Oliveira, P., Stensjö, K., and Lindblad, P. **2011**. 'Chapter Twenty-Four - Synthetic biology in cyanobacteria: Engineering and analyzing novel functions.' in Chris Voigt (ed.), Methods in Enzymology (Academic Press), 497: 539-79.

Hernandez-Prieto, M. A., and Futschik, M. E. **2012**. CyanoEXpress: A web database for exploration and visualisation of the integrated transcriptome of cyanobacterium *Synechocystis* sp. PCC 6803, *Bioinformation*, 8: 634-38.

Hoiczyk, E., and Hansel, A. **2000**. Cyanobacterial cell walls: News from an unusual prokaryotic envelope, *J. Bacteriol.*, 182: 1191-99.

Huang, H.-H., Camsund, D., Lindblad, P., and Heidorn, T. **2010**. Design and characterization of molecular tools for a synthetic biology approach towards developing cyanobacterial biotechnology, *Nucleic Acids Res.*, 38: 2577-93.

Joffe, L. S., Nimrichter, L., Rodrigues, M. L., and Poeta, M. D. **2016**. Potential roles of fungal extracellular vesicles during Infection, *mSphere*, 1: e00099-16.

Kaneko, T., Sato, S., Kotani, H., Tanaka, A., Asamizu, E., Nakamura, Y., Miyajima, N., Hirosawa, M., Sugiura, M., Sasamoto, S., Kimura, T., Hosouchi, T., Matsuno, A., Muraki, A., Nakazaki, N., Naruo, K., Okumura, S., Shimpo, S., Takeuchi, C., Wada, T., Watanabe, A., Yamada, M., Yasuda, M., and Tabata, S. **1996**. Sequence analysis of the genome of the unicellular cyanobacterium *Synechocystis* sp. strain PCC 6803. II. Sequence determination of the entire genome and assignment of potential protein-coding regions, *DNA Res.*, 3: 109-36.

Katoh, H., Hagino, N., Grossman, A. R., and Ogawa, T. **2001**. Genes essential to iron transport in the cyanobacterium *Synechocystis* sp. strain PCC 6803, *J. Bacteriol.*, 183: 2779-84.

Kesty, N. C., and Kuehn, M. J. **2004**. Incorporation of heterologous outer membrane and periplasmic proteins into *Escherichia coli* outer membrane vesicles, *J. Biol. Chem.*, 279: 2069-76.

Kojima, S., Muramoto, K., and Kusano, T. **2016**. Outer membrane proteins derived from non-cyanobacterial lineage cover the peptidoglycan of *Cyanophora paradoxa* cyanelles and serve as a cyanelle diffusion channel, *J. Biol. Chem.*, 291: 20198-209.

Kojima, S., and Okumura, Y. **2020**. Outer membrane-deprived cyanobacteria liberate periplasmic and thylakoid luminal components that support the growth of heterotrophs, *bioRxiv*: 2020.03.24.006684.

Kopf, M., Klähn, S., Scholz, I., Matthiessen, J. K. F., Hess, W. R., and Voß, B. **2014**. Comparative analysis of the primary transcriptome of *Synechocystis* sp. PCC 6803, *DNA Res.*, 21: 527-39.

Kowata, H., Tochigi, S., Takahashi, H., and Kojima, S. **2017**. Outer membrane permeability of cyanobacterium *Synechocystis* sp. strain PCC 6803: Studies of passive diffusion of small organic nutrients reveal the absence of classical porins and intrinsically low permeability, *J. Bacteriol.*, 199: e00371-17.

Krewulak, K. D., and Vogel, H. J. **2008**. Structural biology of bacterial iron uptake, *Biochim. Biophys. Acta-Biomembr.,* 1778: 1781-804.

Kulp, A., and Kuehn, M. J. **2010**. Biological functions and biogenesis of secreted bacterial outer membrane vesicles, *Annu. Rev. Microbiol.*, 64: 163-84.

Lau, N.-S., Matsui, M., and Abdullah, A. A.-A. **2015**. Cyanobacteria: Photoautotrophic microbial factories for the sustainable synthesis of industrial products, *BioMed Res. Int.,* 2015: 754934.

Lima, S., Matinha-Cardoso, J., Tamagnini, P., and Oliveira, P. **2020**. Extracellular vesicles: An overlooked secretion system in cyanobacteria, *Life*, 10: 129.

Lin, J., Zhang, W., Cheng, J., Yang, X., Zhu, K., Wang, Y., Wei, G., Qian, P.-Y., Luo, Z.-Q., and Shen, X. **2017**. A Pseudomonas T6SS effector recruits PQS-containing outer membrane vesicles for iron acquisition, *Nat. Commun.*, 8: 14888.

Mashburn-Warren, L., Howe, J., Garidel, P., Richter, W., Steiniger, F., Roessle, M., Brandenburg, K., and Whiteley, M. **2008**. Interaction of quorum signals with outer membrane lipids: insights into prokaryotic membrane vesicle formation, *Mol. Microbiol.*, 69: 491-502.

Mashburn-Warren, L. M., and Whiteley, M. **2006**. Special delivery: Vesicle trafficking in prokaryotes, *Mol. Microbiol.*, 61: 839-46.

McBroom, A. J., Johnson, A. P., Vemulapalli, S., and Kuehn, M. J. **2006**. Outer membrane vesicle production by *Escherichia coli* is independent of membrane instability, *J. Bacteriol.*, 188: 5385-92.

McBroom, A. J., and Kuehn, M. J. **2007**. Release of outer membrane vesicles by Gram-negative bacteria is a novel envelope stress response, *Mol. Microbiol.*, 63: 545-58.

McDonald, M. K., Tian, Y., Qureshi, R. A., Gormley, M., Ertel, A., Gao, R., Aradillas Lopez, E., Alexander, G. M., Sacan, A., Fortina, P., and Ajit, S. K. **2014**. Functional significance of macrophage-derived exosomes in inflammation and pain, *PAIN*, 155: 1527-39.

McMahon, K. J., Castelli, M. E., Vescovi, E. G., and Feldman, M. F. **2012**. Biogenesis of outer membrane vesicles in *Serratia marcescens* is thermoregulated and can be induced by activation of the *rcs* phosphorelay system, *J. Bacteriol.*, 194: 3241-49.

Mesnage, S., Fontaine, T., Mignot, T., Delepierre, M., Mock, M., and Fouet, A. **2000**. Bacterial SLH domain proteins are non-covalently anchored to the cell surface via a conserved mechanism involving wall polysaccharide pyruvylation, *Embo J.*, 19: 4473-84.

Mills, L. A., McCormick, A. J., and Lea-Smith, D. J. **2020**. Current knowledge and recent advances in understanding metabolism of the model cyanobacterium *Synechocystis* sp. PCC 6803, *Biosci. Rep.*, 40: BSR20193325.

Moon, D. C., Choi, C. H., Lee, J. H., Choi, C.-W., Kim, H.-Y., Park, J. S., Kim, S. I., and Lee, J. C. **2012**. *Acinetobacter baumannii* outer membrane protein A modulates the biogenesis of outer membrane vesicles, *J. Microbiol.,* 50: 155-60.

Mota, R., Vidal, R., Pandeirada, C., Flores, C., Adessi, A., De Philippis, R., Nunes, C., Coimbra, M. A., and Tamagnini, P. **2020**. Cyanoflan: A cyanobacterial sulfated carbohydrate polymer with emulsifying properties, *Carbohydr. Polym.*, 229: 115525.

Noinaj, N., Guillier, M., Barnard T. J., and Buchanan, S. K. **2010**. TonB-dependent transporters: Regulation, structure, and function, *Annu. Rev. Microbiol.,* 64: 43-60.

Oliveira, P., Martins, N. M., Santos, M., Pinto, F., Büttel, Z., Couto, N. A. S., Wright, P. C., and Tamagnini, P. **2016**. The versatile TolC-like Slr1270 in the cyanobacterium *Synechocystis* sp. PCC 6803, *Environ. Microbiol.*, 18: 486-502.

Papanikou, E., Karamanou, S., and Economou, A. **2007**. Bacterial protein secretion through the translocase nanomachine, *Nat. Rev. Microbiol.,* 5: 839-51.

Pardo, Y. A., Florez, C., Baker, K. M., Schertzer, J. W., and Mahler, G. J. **2015**. Detection of outer membrane vesicles in *Synechocystis* PCC 6803, *FEMS Microbiol. Lett.*, 362: fnv163.

Park, J. S., Lee, W. C., Yeo, K. J., Ryu, K.-S., Kumarasiri, M., Hesek, D., Lee, M., Mobashery, S., Song, J. H., Kim, S. I., Lee, J. C., Cheong, C., Jeon, Y. H., and Kim, H.-Y. **2012**. Mechanism of anchoring of OmpA protein to the cell wall peptidoglycan of the gram-negative bacterial outer membrane, *Faseb J.,* 26: 219-28.

Pérez-Cruz, C., Carrión, O., Delgado, L., Martinez, G., López-Iglesias, C., and Mercade, E. **2013**. New type of outer membrane vesicle produced by the Gram-negative bacterium *Shewanella vesiculosa* $M7^T$: Implications for DNA content, *Appl. Environ. Microbiol.*, 79: 1874-81.

Pérez-Cruz, C., Delgado, L., López-Iglesias, C., and Mercade, E. **2015**. Outer-inner membrane vesicles naturally secreted by gram-negative pathogenic bacteria, *PLoS One*, 10: e0116896.

Pinto, F., Pacheco, C. C., Oliveira, P., Montagud, A., Landels, A., Couto, N., Wright, P. C., Urchueguía, J. F., and Tamagnini, P. **2015**. Improving a Synechocystis-based photoautotrophic chassis through systematic genome mapping and validation of neutral sites, *DNA Res.*, 22: 425-37.

Pisciotta, J. M., Zou, Y., and Baskakov, I. V. **2010**. Light-dependent electrogenic activity of cyanobacteria, *PLoS One*, 5: e10821.

Polyviou, D., Machelett, M. M., Hitchcock, A., Baylay, A. J., MacMillan, F., Moore, C. M., Bibby, T. S., and Tews, I. **2018**. Structural and functional characterization of IdiA/FutA (Tery_3377), an iron-binding protein from the ocean diazotroph *Trichodesmium erythraeum*, *J. Biol. Chem.*, 293: 18099-109.

Prados-Rosales, R., Weinrick, B. C., Piqué, D. G., Jacobs, W. R., Casadevall, A., and Rodriguez, G. M. **2014**. Role for Mycobacterium tuberculosis Membrane Vesicles in Iron Acquisition, *J. Bacteriol.*, 196: 1250-56.

Qiu, G.-W., Jiang, H.-B., Lis, H., Li, Z.-K., Deng, B., Shang, J.-L., Sun, C.-Y., Keren, N., and Qiu, B.-S. **2021**. A unique porin meditates iron-selective transport through cyanobacterial outer membranes, *Environ. Microbiol.*, 23: 376-90.

Qiu, G.-W., Lou, W.-J., Sun, C.-Y., Yang, N., Li, Z.-K., Li, D.-L., Zang, S.-S., Fu, F.-X., Hutchins, D. A., Jiang, H.-B., and Qiu, B.-S. **2018**. Outer membrane iron uptake pathways in the model cyanobacterium *Synechocystis* sp. strain PCC 6803, *Appl. Environ. Microbiol.,* 84: e01512-18.

Roier, S., Zingl, F. G., Cakar, F., Durakovic, S., Kohl, P., Eichmann, T. O., Klug, L., Gadermaier, B., Weinzerl, K., Prassl, R., Lass, A., Daum, G., Reidl, J., Feldman, M. F., and Schild, S. **2016**. A novel mechanism for the biogenesis of outer membrane vesicles in Gram-negative bacteria, *Nat. Commun.*, 7: 10515

Russo, D. A., Zedler, J. A. Z., Wittmann, D. N., Möllers, B., Singh, R. K., Batth, T. S., van Oort, B., Olsen, J. V., Bjerrum, M. J., and Jensen, P. E. **2019**. Expression and secretion of a lytic polysaccharide monooxygenase by a fast-growing cyanobacterium, *Biotechnol. Biofuels*, 12: 74.

Sager , R., and Palade , G. E. **1957**. Structure and development of the chloroplast in *Chlamydomonas*: I. The normal green cell, *J. Biophys. and Biochem. Cytol.*, 3: 463-88.

Schertzer, J. W., and Whiteley, M. **2012**. A bilayer-couple model of bacterial outer membrane vesicle biogenesis, *mBio*, 3: e00297-11.

Schneider, C. A., Rasband, W. S., and Eliceiri, K. W. **2012**. NIH Image to ImageJ: 25 years of image analysis, Nat. Methods, 9: 671-75.

Schwechheimer, C., and Kuehn, M. J. **2015**. Outer-membrane vesicles from Gram-negative bacteria: biogenesis and functions, *Nat. Rev. Microbiol.*, 13: 605-19.

Schwechheimer, C., Kulp, A., and Kuehn, M. J. **2014**. Modulation of bacterial outer membrane vesicle production by envelope structure and content, *BMC Microbiol.*, 14: 324.

Sciuto, K., and Moro, I. **2015**. Cyanobacteria: The bright and dark sides of a charming group, *Biodivers. Conserv.*, 24: 711-38.

Silhavy, T. J., Kahne, D., and Walker, S. **2010**. The bacterial cell envelope, *Cold Spring Harb. Perspect. Biol.*, 2: a000414.

Sleytr, U. B., Schuster, B., Egelseer, E.-M., and Pum, D. **2014**. S-layers: Principles and applications, *Fems Microbiol. Rev.*, 38: 823-64.

Smith, S. G. J., Mahon, V., Lambert, M. A., and Fagan, R. P. **2007**. A molecular Swiss army knife: OmpA structure, function and expression, *FEMS Microbiol. Lett.*, 273: 1-11.

Song, T., Mika, F., Lindmark, B., Liu, Z., Schild, S., Bishop, A., Zhu, J., Camilli, A., Johansson, J., Vogel, J., and Wai, S. N. **2008**. A new *Vibrio cholerae* sRNA modulates colonization and affects release of outer membrane vesicles, *Mol. Microbiol.*, 70: 100-11.

Sotelo , J. R., and Porter , K. R. **1959**. An electron microscope study of the rat ovum, *J. Biophys. Biochem. Cytol.*, 5: 327-42.

Stanier, R. Y., Kunisawa, R., Mandel, M., and Cohen-Bazire, G. **1971**. Purification and properties of unicellular blue-green algae (order Chroococcales), *Bacteriol. Rev.*, 35: 171-205.

Tamagnini, P., Troshina, O., Oxelfelt, F., Salema, R., and Lindblad, P. **1997**. Hydrogenases in *Nostoc* sp. strain PCC 73102, a strain lacking a bidirectional enzyme, *Appl. Environ. Microbiol.*, 63: 1801-07.

Tietze, L., and Lale, R. **2021**. Importance of the 5′ regulatory region to bacterial synthetic biology applications, *Microb. Biotechnol.*, 14: 2291-315.

Tölle, J., Michel, K.-P., Kruip, J., Kahmann, U., Preisfeld, A., and Pistorius, E. K. **2002**. Localization and function of the IdiA homologue Slr1295 in the cyanobacterium *Synechocystis* sp. strain PCC 6803, Microbiology, 148: 3293-305.

Toyofuku, M., Nomura, N., and Eberl, L. **2019**. Types and origins of bacterial membrane vesicles, *Nat. Rev. Microbiol.*, 17: 13-24.

Trias, J., Rosenberg, E. Y., and Nikaido, H. **1988**. Specificity of the glucose channel formed by protein D1 of *Pseudomonas aeruginosa*, *Biochim. Biophys. Acta - Biomembr.*, 938: 493-96.

Turnbull, L., Toyofuku, M., Hynen, A. L., Kurosawa, M., Pessi, G., Petty, N. K., Osvath, S. R., Cárcamo-Oyarce, G., Gloag, E. S., Shimoni, R., Omasits, U., Ito, S., Yap, X., Monahan, L. G., Cavaliere, R., Ahrens, C. H., Charles, I. G., Nomura, N., Eberl, L., and Whitchurch, C. B. **2016**. Explosive cell lysis as a mechanism for the biogenesis of bacterial membrane vesicles and biofilms, *Nat. Commun.*, 7: 11220.

Turner, L., Praszkier, J., Hutton, M. L., Steer, D., Ramm, G., Kaparakis-Liaskos, M., and Ferrero, R. L. **2015**. Increased outer membrane vesicle formation in a *Helicobacter pylori tolB* mutant, *Helicobacter*, 20: 269-83.

Whitfield, C., and Trent, M. S. **2014**. Biosynthesis and export of bacterial lipopolysaccharides, *Annu. Rev. Biochem.*, 83: 99-128.

Woith, E., Fuhrmann, G., and Melzig, M. F. **2019**. Extracellular vesicles—connecting kingdoms, *Int. J. Mol. Sci.*, 20: 5695.

Xu, Y., Guerra, L. T., Li, Z., Ludwig, M., Dismukes, G. C., and Bryant, D. A. **2013**. Altered carbohydrate metabolism in glycogen synthase mutants of *Synechococcus* sp. strain PCC 7002: Cell factories for soluble sugars, *Metab. Eng.*, 16: 56-67.

Yegorov, Y., Sendersky, E., Zilberman, S., Nagar, E., Ben-Asher, H. W., Shimoni, E., Simkovsky, R., Golden, S. S., LiWang, A., and Schwarz, R. **2021**. A cyanobacterial component required for pilus biogenesis affects the exoproteome, *mBio*, 12: e03674-20.

Yu, Y., You, L., Liu, D., Hollinshead, W., Tang, Y. J., and Zhang, F. **2013**. Development of *Synechocystis* sp. PCC 6803 as a phototrophic cell factory, *Mar. Drugs*, 11: 2894-916.

Zavan, L., Bitto, N. J., and Kaparakis-Liaskos, M. **2020**. 'Introduction, history, and discovery of bacterial membrane vesicles.' in Maria Kaparakis-Liaskos and Thomas A. Kufer (eds.), *Bacterial membrane vesicles: Biogenesis, functions and applications* (Springer International Publishing: Cham), 1-21.

Zhang, X., Betterle, N., Martinez, D. H., and Melis, A. **2021**. Recombinant protein stability in cyanobacteria, *ACS Synth. Biol.*, 10: 810-25.

Zhou, L., Srisatjaluk, R., Justus, D. E., and Doyle, R. J. **1998**. On the origin of membrane vesicles in Gram-negative bacteria, *FEMS Microbiol. Lett.*, 163: 223-28.

Zingl, F. G., Leitner, D. R., and Schild, S. **2020**. 'Biogenesis of Gram-negative OMVs.' in Maria Kaparakis-Liaskos and Thomas A. Kufer (eds.), *Bacterial membrane vesicles: Biogenesis, functions and applications* (Springer International Publishing: Cham), 23-46.